The Abdus Salam
International Centre for Theoretical Physics

United Nations
Educational, Scientific
and Cultural Organization

International Atomic
Energy Agency

SMR.1676 - 37

8th Workshop on Non-Linear Dynamics and Earthquake Prediction

3 - 15 October, 2005

Buoyancy-Driven Contemporary Tectonic Stress & Intermediate-Depth Seismicity in Europe

Ali Ismail-Zadeh
Russian Academy of Sciences
International Inst. of Earthquake Prediction Theory and Matematical Geophysics
Warshavskoye Sh. 79. Kor2
117556 Moscow
Russia

Strada Costiera 11, 34014 Trieste, Italy - Tel. +39 040 2240 111; Fax +39 040 224 163 - sci_info@ictp.it, www.ictp.it

United Nations Educational Scientific and Cultural Organization
and
International Atomic Energy Agency

THE ABDUS SALAM
INTERNATIONAL CENTRE FOR THEORETICAL PHYSICS

Eight Workshop
“Non-Linear Dynamics and Earthquake Prediction”
2 October to 15 October 2005

BUOYANCY-DRIVEN CONTEMPORARY TECTONIC STRESS AND INTERMEDIATE-DEPTH SEISMICITY IN EUROPE

Alik T. Ismail-Zadeh

Geophysical Institute, University of Karlsruhe,
Hertzsrt. 16, Karlsruhe 76187, Germany.
E-mail: Alik.Ismail-Zadeh@gpi.uni-karlsruhe.de

International Institute of Earthquake Prediction Theory and
Mathematical Geophysics, Russian Academy of Sciences,
Warshavskoye shosse 79-2, Moscow 113556, Russia.
E-mail: aismail@mitp.ru

MIRAMARE-TRIESTE
October 2005

Available online at www.sciencedirect.com

SCIENCE DIRECT®

Physics of the Earth and Planetary Interiors 149 (2005) 81–98

PHYSICS OF THE EARTH AND PLANETARY INTERIORS

www.elsevier.com/locate/pepi

Three-dimensional numerical modeling of contemporary mantle flow and tectonic stress beneath the earthquake-prone southeastern Carpathians based on integrated analysis of seismic, heat flow, and gravity data

Alik Ismail-Zadeh[a,b,c,*], Birgit Mueller[a], Gerald Schubert[c]

[a] *Geophysical Institute, University of Karlsruhe, Hertzstr. 16, Karlsruhe 76187, Germany*

[b] *International Institute of Earthquake Prediction Theory and Mathematical Geophysics, Russian Academy of Sciences, Warshavskoye shosse 79-2, Moscow 117556, Russia*

[c] *Department of Earth and Space Sciences and Institute of Geophysics and Planetary Physics, UCLA, 3806 Geology Building, 595 Charles Young Drive East, Los Angeles, CA 90095-1567, USA*

Received 22 August 2003; received in revised form 30 January 2004; accepted 26 August 2004

Abstract

The principal purpose of the study is to understand the interplay between intermediate-depth large earthquakes in the southeastern Carpathians (Vrancea) and tectonic stress induced by a high-velocity body (lithospheric slab) descending into the mantle beneath the region. To analyze processes of stress generation and localization in and around the descending slab, we develop a three-dimensional (3D) numerical model of contemporary mantle flow and stress beneath the Vrancea region. The input data of the model consist of: (i) temperatures derived from seismic P-wave velocity anomalies and surface heat flow, (ii) crustal and uppermost mantle densities converted from P-wave velocities obtained from seismic refraction studies, (iii) geometry of the Vrancea crust and slab from tomography and refraction seismic data, and (iv) the estimated strain rate in the slab (as a result of earthquakes) to constrain the model viscosity. We find that major crustal uplifts predicted by the model coincide with the East Carpathian orogen and surround the Transylvanian basin and that predicted areas of subsidence are associated with the Moesian and East European platforms. We show a correlation between the location of intermediate-depth earthquakes and the predicted localization of maximum shear stress. Modeled tectonic stresses predict large horizontal compression at depths of about 70–220 km beneath the Vrancea region, which coincides with the stress regime defined from fault-plane solutions for the intermediate-depth earthquakes. This implies that buoyancy-driven descent of the lithospheric slab beneath the Vrancea region is directly linked to intermediate-depth seismicity.

Keywords: High-velocity body; Lithospheric slab; Viscous stress; Mantle flow; Numerical modeling; Vrancea seismicity

* Corresponding author. Tel.: +49 721 6084610; fax: +49 721 71173.
E-mail addresses: Alik.Ismail-Zadeh@gpi.uka.de, aismail@mitp.ru (A. Ismail-Zadeh), Birgit.Mueller@gpi.uka.de (B. Mueller), schubert@ucla.edu (G. Schubert).

0031-9201/$ – see front matter
doi:10.1016/j.pepi.2004.08.012

1. Introduction: seismicity and geodynamics of the SE-Carpathians

Repeated large intermediate-depth earthquakes of the southeastern (SE) Carpathians (Vrancea region) cause destruction in Bucharest (Romania) and shake central and eastern European cities several hundred kilometers away from the hypocenters of the events. The earthquake-prone Vrancea region is situated at the bend of the SE-Carpathians and is bounded to the north and north-east by the Eastern European platform (EEP), to the east by the Scythian platform (SP), to the south-east by the Dobrogea orogen (DO), to the south and south-west by the Moesian platform (MP), and to the north-west by the Transylvanian basin (TB). The epicenters of the mantle earthquakes in the Vrancea region are concentrated within a very small area (Fig. 1). The projection of the foci on a NW–SE vertical plane across the bend of the eastern Carpathians (section AB in Fig. 1) shows a seismogenic volume about 110 km (deep) × 70 km × 30 km, and extending to a depth of about 180 km. Beyond this depth, the seismicity ends suddenly: one seismic event at 220 km depth represents an exception (Oncescu and Bonjer, 1997). According to the historical catalogue of Vrancea events (Radu, 1979, 1991), large intermediate-depth shocks with magnitudes $M_W > 6.5$ occur three to five times per century. In the 20th century, large events at depths d of 70–180 km occurred in 1940 (moment magnitude $M_W = 7.7$, $d = 160$ km), in 1977 ($M_W = 7.5$, $d = 100$ km), in 1986 ($M_W = 7.2$, $d = 140$ km), and in 1990 ($M_W = 6.9$, $d = 80$ km) (e.g., Oncescu and Bonjer, 1997).

The 1940 earthquake gave rise to the development of a number of geodynamic models for this region. Gutenberg and Richter (1954) drew attention to the Vrancea region as a place of remarkable intermediate-depth seismicity. Later McKenzie (1972) suggested that this seismicity is associated with a relic slab sinking in the mantle and now overlain by continental crust. The 1977 disastrous earthquake and later the 1986 and 1990 earthquakes again raised questions about the nature of the earthquakes. A seismic gap at depths of 40–70 km beneath Vrancea led to the assumption that the lithospheric slab had already detached from the continental crust (Fuchs et al., 1979). Oncescu (1984) proposed

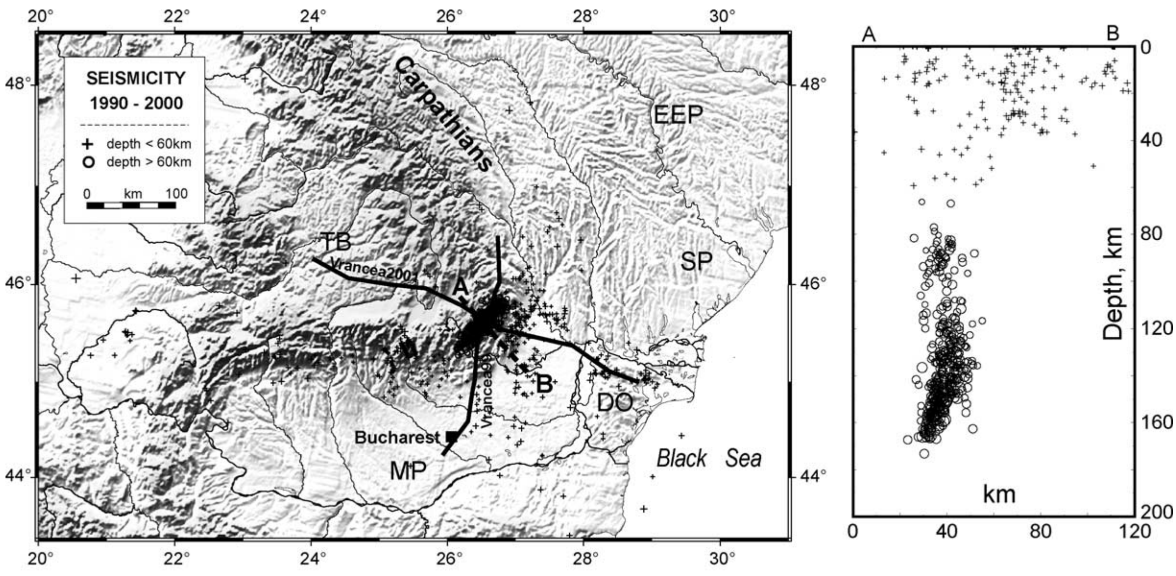

Fig. 1. Observed seismicity in Romania for the last decade with magnitude $M_W \geq 3$ (after Oncescu and Bonjer, 1997; Sperner et al., 2001). (a) Epicenters of Vrancea earthquakes determined by the joint hypocenter method. The background is the topography; the two bold lines show the location of the refraction seismic profiles VRANCEA99 (N–S) and VRANCEA2001 (E–W). (b) Hypocenters of the same earthquakes projected onto the NW–SE vertical plane AB (dashed line in (a)). DO, Dobrogea orogen; EEP, Eastern European platform; MP, Moesian platform; SP, Scythian platform; and TB, Transylvanian basin.

that the intermediate-depth events are generated in a zone that separates the sinking slab from the neighboring immobile part of the lithosphere rather than in the sinking slab itself. Linzer (1996) explained the nearly vertical position of the Vrancea slab as the final rollback stage of a small fragment of oceanic lithosphere, and Girbacea and Frisch (1998) assumed that the break-off, affecting only the crustal portion of the slab, was followed by horizontal delamination of its lower portion. Most recently, Sperner et al. (2001) suggested a model of Miocene subduction of oceanic lithosphere beneath the Carpathian arc and subsequent soft continental collision, which transported cold and dense lithospheric material into the mantle. While Linzer (1996), Girbacea and Frisch (1998), and Sperner et al. (2001) consider the slab to be oceanic, its origin is still under debate: whether the descending lithosphere is oceanic or continental. Pana and Erdmer (1996) and Pana and Morris (1999) argue that there is no geological evidence of Mesozoic oceanic crust in the eastern Carpathians and the descending lithosphere is likely to be thinned continental or transitional.

Continental convergence in the SE-Carpathians ceased about 10 Ma (Jiricek, 1979; Csontos et al., 1992). Initially, flat subduction zone began to steepen to its present nearly vertical orientation (Sperner, CRC 461 Team, 2004). At present the cold slab (hence, denser than the surrounding mantle) beneath the Vrancea region sinks due to gravity. The hydrostatic buoyancy forces promote the sinking of the slab, but viscous and frictional forces resist the descent. The combination of these forces produces shear stresses at intermediate depths that are high enough to cause earthquakes. This was shown in two-dimensional (2D) numerical models of mantle flow and tectonic stress by Ismail-Zadeh et al. (2000). These authors recognized that the depth distribution of the annual average seismic energy released in earthquakes has a shape similar to that of the depth distribution of the modeled stress magnitude in the slab.

Hettel et al. (2000) presented a simplified finite-element model of the descending viscoelastic slab and showed the onset of a necking process in the slab and decoupling between the slab and the overlying lithosphere. To evaluate the role of slab detachment in stress evolution, Ismail-Zadeh et al. (2004) developed two-dimensional thermo-mechanical finite-element models of the post-Miocene subduction of the Vrancea slab subject to gravity forces alone. The models predicted lateral compression in the slab that were in agreement with those inferred from the stress axes of earthquakes. It was found that the maximum stress occurs in the depth range of 80–200 km and the minimum stress falls into the depth range of 40–80 km, which corresponds to the seismic gap. It was also shown that high tectonic stress (leading to seismic activity) is preserved in the slab for a few million years, even after the detachment. The two-dimensional numerical studies revealed principal features of mantle flow and tectonic stresses induced by a simple model of the descending slab, but they could not show a correlation between the descending high-velocity body, tectonic stress, and the locations of the Vrancea intermediate-depth earthquakes in any detail.

The principal purposes of this research are to understand (i) how the uppermost mantle structure beneath the SE-Carpathians relates to the intermediate-depth seismicity in the Vrancea region and (ii) how these seismic events correlate with the tectonic stresses induced by the descending high-velocity body (lithospheric slab) observed in the seismic tomography experiment. Hence, we develop a three-dimensional (3D) numerical finite-element model of the instantaneous viscous flow and tectonic stress in the region where input model parameters (geometry, temperature, density, viscosity) are based on the results of regional seismic tomography, seismic refraction studies, and the subsequent modeling of density, gravity, and temperature. The model does not require knowledge of the origin of the Vrancea slab and uses only the data obtained from experiments and natural observations.

We summarize the results of the recent seismic tomographic study conducted in the SE-Carpathians in Section 2.1, the results of two international projects on seismic refraction studies in the region in Section 2.2, the results of the density modeling in the SE-Carpathians and of the regional gravity modeling in Section 3. We discuss possibilities for deriving temperature of the mantle (Section 4.1) and crust (Section 4.2) from the seismic and heat flow data and present results of the temperature modeling beneath the SE-Carpathians. The model of mantle and crustal flow and of tectonic stress in the region is described in Section 5.1, the predicted flow in Section 5.2, and tectonic stress in Section 5.3. Then, we discuss the model results, the limitations and uncertainties of the study, and conclude the research.

2. Seismic studies of the SE-Carpathians

2.1. Seismic tomography

In 1999, the international tomographic experiment CALIXTO with 143 seismic stations was conducted in southeastern Romania (Martin et al., 2001). During the field experiment 160 local events with magnitude $M_l \geq 2.0$ and 450 teleseismic events with magnitude $M_b \geq 5.0$ were recorded. The distance between stations ranged from 15–20 km (the Vrancea region) to 25–30 km (outer margins of the network), covering a region of about 350 km in diameter. First results were achieved through an inversion of the teleseismic data with the ACH method (Aki et al., 1977; Evans and Achauer, 1993). Crustal complexity causes a smearing of these results for the upper 60 km. This can be overcome if travel times are calculated through a realistic regional crustal model (Martin, 2003). Variations in crustal thickness, and young deep basins, like the Focsani foredeep basin with its 9 km of Neogene to Quaternary sediments, have to be considered. In such a more sophisticated analysis, the boundaries of the anomalies might shift by at most 20 km. Nevertheless, the results for the deeper parts are reliable enough for the present study to fix the general shape of the velocity anomalies.

Data inversion reveals a high-velocity body with maximum P-wave velocity perturbations of +3.5% in comparison with the background model (see Fig. 2). This high-velocity body is interpreted as the descending lithospheric slab. It reaches a depth of at least 350 km (this is a maximum depth of high resolution tomography), which is in good agreement with results of previous seismic tomography studies (e.g., Wortel and Spakman, 2000). The tomography images reveal features not visible in previous studies by Oncescu (1984), Wenzel et al. (1999), and Bijwaard and Spakman (2000), and allow determination of the geometry of the descending slab and its spatial relation to the earthquake hypocenters (the latter are confined to the southeastern margin of the slab). The slab extends to the south-west beneath the Moesian platform, however this portion of the slab is completely aseismic (Fig. 2).

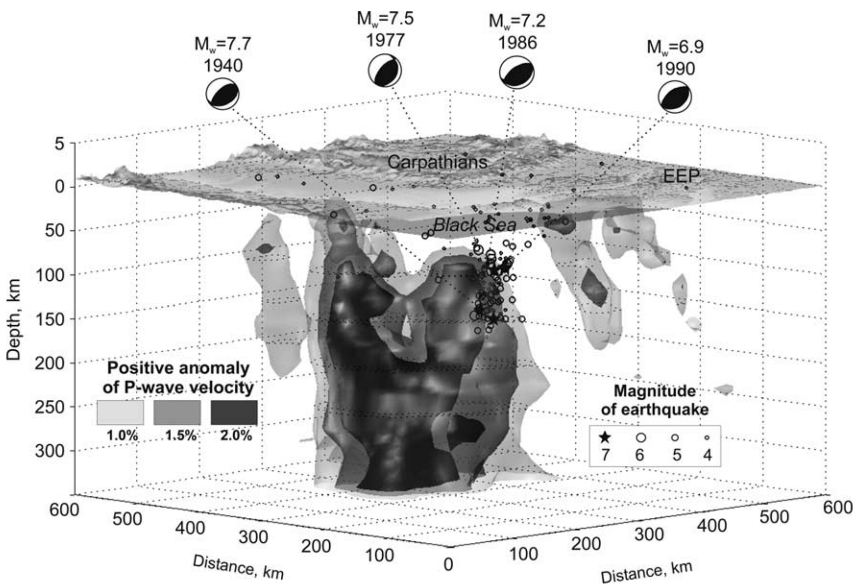

Fig. 2. Seismic tomographic image of the Vrancea slab (Martin et al., 2001) and hypocenters of earthquakes (circles and asterisks indicate the location and magnitude of seismic events). Three shaded grey surfaces represent the surfaces of 1, 1.5, and 2% positive anomalies of P-wave velocity obtained via teleseismic data inversion. The top surface illustrates the topography. Focal spheres are fault plane solutions for the four largest Vrancea intermediate-depth earthquakes in the 20th century.

Sperner, CRC 461 Team (2004) considers this aseismic portion to be already delaminated from the overlying lithosphere.

Because the upper part of the high-velocity body cannot presently be defined from the seismic tomography images, we use the results of the refraction seismic investigations in our analysis.

2.2. Seismic refraction study

Two active-source seismic experiments (in 1999 and 2001) were carried out in the SE-Carpathians to study the crustal and uppermost mantle structure and physical properties beneath the Vrancea region (Hauser et al., 2001, 2002). The 300 km long VRANCEA99 and the 460 km long VRANCEA2001 seismic refraction profiles crossed the Vrancea epicentral area in NNE–SSW and ESE–WNW directions, respectively (Fig. 1). From forward and inverse ray trace modeling, Hauser et al. (2001, 2002) distinguished a multi-layered crust with lateral velocity variations in the sedimentary cover and minor changes in the crystalline crust. They showed that the sedimentary succession comprises two to four seismic layers of variable thickness with velocities ranging from 2.0 to 5.8 km s^{-1}. The upper part of the seismic basement coincides with a velocity of 5.9 km s^{-1}; velocities in the upper crystalline crust are 5.9–6.2 km s^{-1}. An intra-crustal discontinuity apparent at depths between 18 and 31 km divides the crust into an upper and a lower layer.

The Moho discontinuity is predicted at a depth of about 40 km near the intersection of these profiles. Hauser et al. (2002) reported that the Moho shows no crustal roots under the Carpathians. Velocities are 6.7–7.0 km s^{-1} within the lower crust and about 7.9 km s^{-1} just below the Moho. Hauser et al. (2001) found a low-velocity zone (7.6 km s^{-1}) within the uppermost part of the mantle (at depths of 45–55 km) and the velocity beneath this zone is at least 8.5 km s^{-1}. This low velocity zone is situated within the area of the seismic gap at depths of 40–70 km (Oncescu, 1984).

3. Density and gravity modeling

Based on the seismic velocity models obtained from the refraction experiments and seismic tomography, we derived a 3D density model using the empirical velocity (v_P) to density (ρ) relationships developed by Krasovsky (1989):

$$\rho\,[\mathrm{kg\,m^{-3}}] = 10^3(0.7212 + 0.3209 v_P\,[\mathrm{km\,s^{-1}}])$$

Krasovsky (1989) summarized and processed experimental data on this relationship at high pressures for more than 2000 samples of various crystalline rocks worldwide taking into consideration the rock composition and metamorphic grade.

On the basis of the derived density models, Hackney et al. (2002) developed a 3D gravity model of the SE-Carpathians employing the IGMAS software for gravity modeling (Schmidt and Götze, 1998). It was shown that the gravity effect predicted for the Vrancea slab is about +20 mGal. When the slab gravity effect is removed from the observed Bouguer anomalies (Ioane and Atanasiu, 1998), the signature associated with the Carpathian foredeep (most negative Bouguer anomalies) is more negative. Hackney et al. (2002) suggested that this modified anomaly pattern might better reflect the geometry of the foredeep basin.

4. Temperature modeling

Temperature is a key physical parameter controlling the density, viscosity, and rheology of the Earth's material and hence crustal and mantle dynamics. Information on temperature inside the Earth's shallow crust comes from direct measurements of temperature in boreholes. There are however no direct measurements of deep crustal and mantle temperatures, and therefore the temperatures can be estimated indirectly from either seismic wave anomalies, geochemical analysis or through the extrapolation of surface heat flow observations.

4.1. Mantle temperatures from P-wave tomography

Seismic waves allow for 3D imaging of seismic velocities of the Earth's interior. The seismic velocity anomalies in the upper mantle can be attributed to variations in temperature (Forte et al., 1994, 1995), although several factors other than temperature can also exert an influence on seismic velocity: composition (Griffin et al., 1998), anelasticity (Karato, 1993), anisotropy, and presence of melt or water (Karato, 2004). Uppermost mantle composition has a complex effect on seismic velocity, while the effect is relatively small compared to the effect of temperature (Jordan, 1979; Sobolev et al., 1996; Goes et al., 2000). During peridotite melting, garnet and clinopyroxene (fastest and slowest of four major minerals which compose the upper mantle) concentrate in the melt (Niu, 1997), and therefore the change in composition of peridotite, as it melts and the melt is extracted, does not appear to significantly affect seismic velocities (Jordan, 1979). Meanwhile the presence of melt may have an effect on seismic velocities.

Seismic wave velocities are affected by melting depending on the melt fraction and geometry. Takei (2000) and Hammond and Humphreys (2000a,b) showed that for a reasonable range of geometries, partial melting has an important effect on seismic wave velocities when the melt fraction exceeds ∼1%. The melt fraction for a given material is controlled by the degree of partial melting and the efficiency of melt transport, and the degree of partial melting is determined by temperature and water content. Interpretation of seismic anisotropy is not always unique because of a trade-off between mantle flow geometry and physical mechanisms of anisotropic structure formation (e.g., Smith et al., 2001). Therefore, in the forward modeling of synthetic P-wave seismic velocity anomalies beneath the SE-Carpathians the effects of anharmonicity (composition), anelasticity, and partial melting on seismic velocities were considered.

The seismic tomographic model of the SE-Carpathians we used to derive temperature consists of nine layers of different thickness, which are each subdivided into rectangular blocks (Martin et al., 2001). To restrict numerical errors in the subsequent analysis of flow and tectonic stress we smooth the velocity anomaly data using spline interpolations between the blocks and the layers.

The anharmonic (frequency independent and non-attenuating) part of the synthetic velocities was calculated on the basis of published data on laboratory measurements of density and elastic parameters of the main rock-forming minerals (e.g., Bass, 1995) at various thermodynamic conditions for the composition of the crust and mantle (57.9% Ol, 16.3% CPx, 13.5% Opx, and 12.3% Gt; Green and Falloon, 1998) and the slab (69% Ol, 10% CPx, 19% Opx, and 2% Gt; Agee, 1993). The methodology described by Goes et al. (2000) was used to derive the anharmonic part of the synthetic velocities. To evaluate the effects of anelasticity (attenuation and frequency dependence) and melting, a methodology similar to Sobolev et al. (1996) was employed. Once the synthetic velocities are calculated for a first-guess temperature, an iteration process is used to find the 'true' temperature, minimizing the difference between the synthetic and 'observed' (in seismic tomography experiments) velocities. During the conversion of seismic velocity to temperature, the reference (background) temperature should be introduced. The laterally averaged temperature in the crust and mantle modeled by Demetrescu and Andreescu (1994) was chosen as the background temperature for this inversion (Fig. 3).

The mantle temperatures at depths of 90, 120, 150, and 200 km are presented in Fig. 4. The pattern of resulting mantle temperature anomalies (predicted temperature minus background temperature) is similar to the pattern of observed P-wave velocity anomalies (Martin et al., 2001), but does not exactly mimic it because of the non-linear inversion of P-wave velocity anomalies to temperature. The modeled low mantle temperatures are associated with the high-velocity

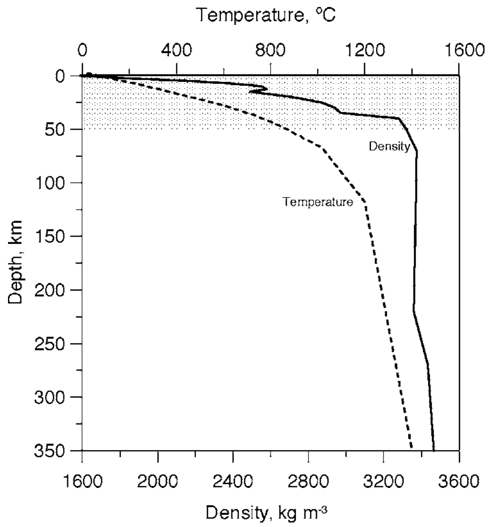

Fig. 3. Density and temperature vs. depth used as the background parameters in the modeling. Density curve: the laterally averaged density obtained from the P-wave velocity to density relationship (Krasovsky, 1989) for the 50-km upper layer of the model (shaded zone) and the density derived from PREM for the rest of the model domain. Temperature curve: the laterally averaged temperature (Demetrescu and Andreescu, 1994).

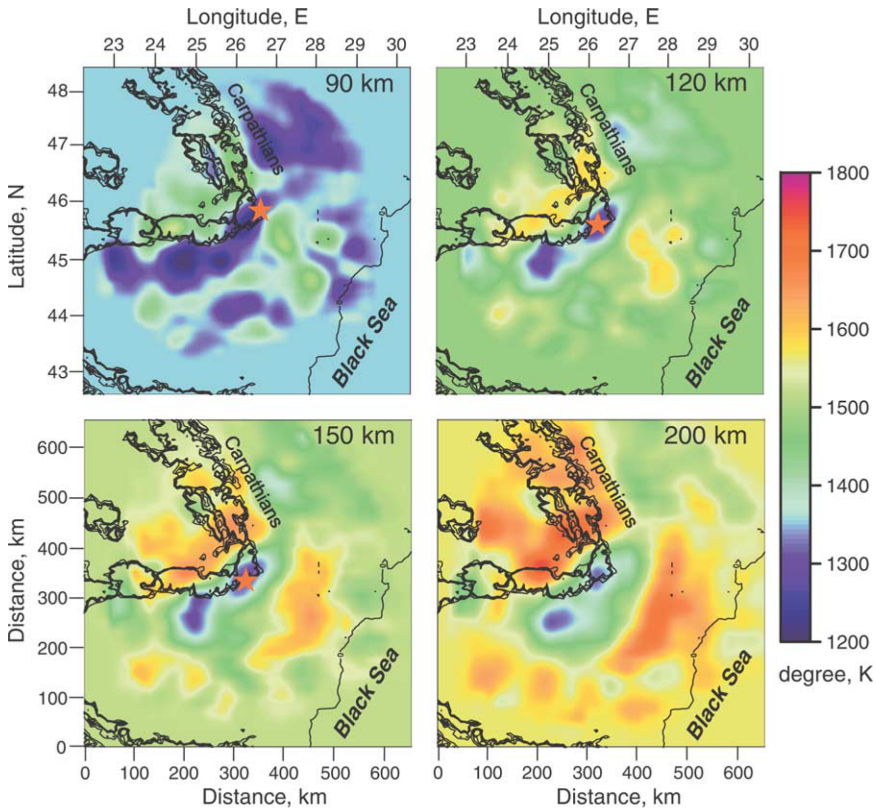

Fig. 4. Temperatures derived from P-wave velocity anomalies beneath the SE-Carpathians at different depths in the mantle. The composition, anharmonicity, anelasticity, and partial melting are taken into account. Isolines present the surface topography. Star shows the location of the Vrancea intermediate-depth earthquakes.

body beneath the Vrancea region and the lithosphere of the East European platform. High temperatures are predicted beneath the Transylvanian depression, the regions of Neogene magmatism in the eastern Carpathians, and the Dobrogea orogen.

4.2. *Crustal and uppermost mantle temperatures from heat flow*

Smearing of the results of seismic tomography for the upper 60 km does not allow correct prediction of the temperature in the crust and uppermost mantle. The temperature in the shallow levels of the Romanian region was modeled from measured surface heat flux corrected for paleoclimate changes in the last 70,000 years (+8 mW m^{-2}) and for the effects of sedimentation on temperatures in the crust in the Focsani and Transylvanian depressions (Demetrescu et al., 2001). A 1D temperature distribution with depth was calculated starting from the measured surface heat flux, assuming steady-state conduction of heat through the lithosphere and adopting a certain model of thermal parameters (thermal conductivity and heat production) characterizing the various subdivisions of the crust and upper mantle. The analytical solution to the steady-state conduction equation of the heat transfer in a multi-layered medium was used (Demetrescu and Andreescu, 1994).

Fig. 5 presents the temperatures at depths of 20 and 50 km. The high temperatures beneath the Neogene volcanic area (25–26°E, 46–47°N) are associated with the high surface heat flux (>80 mW m^{-2}). Depending on the crustal model adopted for the volcanic activity (in the presence or absence of magma chambers with high temperature in the crust), temperatures might differ in the depth range of 20–50 km. The temperatures presented in Fig. 5 come from a model without magma

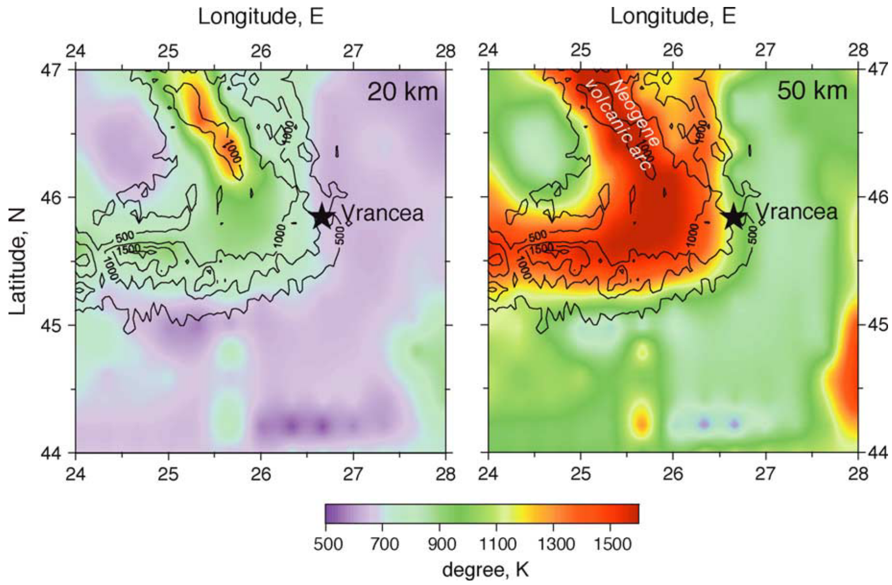

Fig. 5. Temperature in the crust (left; after Demetrescu and Andreescu, 1994) and subcrustal mantle (right; Demetrescu and Andreescu, unpublished data) estimated from the surface heat flux in the region. Isolines present the surface topography. Star shows the location of the Vrancea intermediate-depth earthquakes.

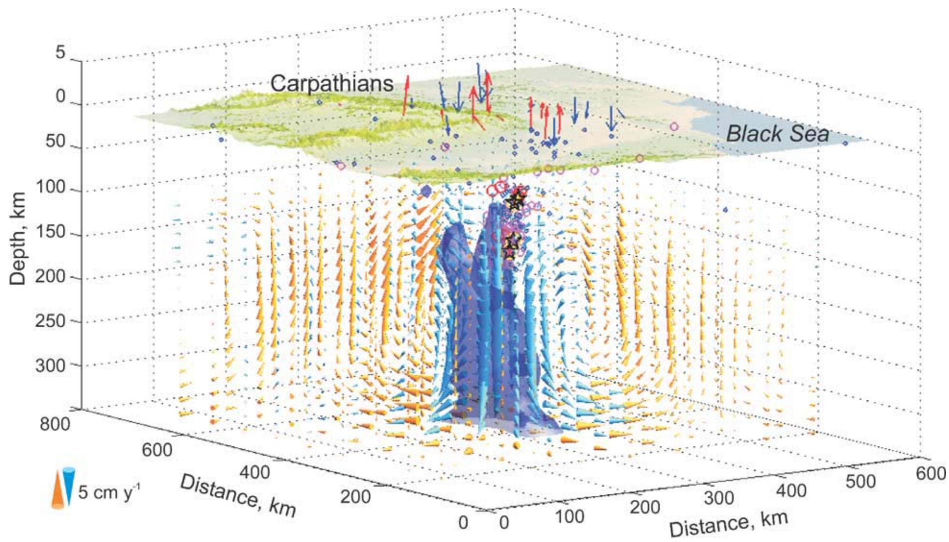

Fig. 6. Predicted contemporary flow induced by the descending slab beneath the SE-Carpathians. Cones illustrate the direction and magnitude of the flow. The violet surface in the middle of the model domain is the surface of 2% positive P-wave velocity anomaly (modeled slab). The top surface is the topography. Arrows on the top of the surface topography are GPS data on the vertical movements in the Vrancea region (Dinter et al., 2001). Circles ($M_W < 6.5$) and asterisks ($M_W > 6.5$) mark the hypocenters of the Vrancea earthquakes.

chambers in the crust (C. Demetrescu, personal communication).

5. Mantle flow and stress

5.1. Model description

To study the effects of the slab on tectonic stress in the region, we develop a 3D numerical model of the descending Vrancea slab based on realistic (in the sense of the seismic tomographic image) slab geometry. We consider the model interface between the Vrancea slab and the surrounding mantle to coincide with the surface of 2% positive anomaly of P-wave seismic velocity obtained in the regional seismic tomography study (see Fig. 2). The interface between the crust and mantle in the model is a 3D extrapolation of the Moho discontinuity found in the seismic refraction studies (Hauser et al., 2001, 2002). The model structure comprises the crust, slab, and uppermost mantle (down to 350 km depth). With respect to our 2D numerical analysis of tectonic stress (Ismail-Zadeh et al., 2000, 2004), which assumed a simplified geometry and physical parameters, we now add some complexities such as the realistic geometry, temperature distribution based on seismic and heat flow data, temperature-dependent density, and temperature- and pressure-dependent viscosity. These complexities permit a more detailed comparison between model predictions and observations.

In the model domain, Ω: $\{0 \le x_1 \le l_1,\ 0 \le x_2 \le l_2,\ 0 \le x_3 \le l_3\}$ (where $\mathbf{x} = (x_1, x_2, x_3)$ are the Cartesian coordinates), we consider an inhomogeneous viscous mantle flow in the presence of gravity. The flow is described by the momentum (Stokes) equation

$$-\nabla P + \mathrm{div}\{\mu(T, P)e_{ij}\} + \rho(T)g = 0, \tag{1}$$

the incompressibility condition

$$\mathrm{div}\,\mathbf{u} = 0, \tag{2}$$

the equation of state for density

$$\rho(T) = \rho_*(x_3)[1 - \alpha(T - T_*)], \tag{3}$$

and the temperature- and pressure-dependent viscosity

$$\mu(T, P) = \mu_*(x)\exp\left(\frac{E + PV}{RT} - \frac{E + P_0 V}{RT_*}\right), \tag{4}$$

where P is the pressure, μ the viscosity, ρ the density, T the temperature, $\mathbf{u} = (u_1, u_2, u_3)$ the flow velocity, $e_{ij} = 0.5(\partial u_i/\partial x_j + \partial u_j/\partial x_i)$ the strain-rate tensor, g the acceleration due to gravity, α the coefficient of thermal expansion, P_0 pressure at the surface, E the activation energy, V the activation volume, R the universal gas constant, and $\rho_*(x_3)$, $\mu_*(\mathbf{x})$, and $T_*(x_3)$ are the background density, viscosity, and temperature, respectively. While the dynamics of the descending slab is described mathematically also by the heat balance equation, we do not employ the latter equation in this modeling, because we compute the instantaneous flow and tectonic stress.

We consider laterally averaged densities in the crust and subcrustal mantle derived from the P-wave velocities (see Table 1 and Fig. 3) as the background density $\rho_*(x_3)$ for the 50-km upper layer of the model. The background density for the modeled mantle is based on the PREM model (Dziewonski and Anderson, 1981). The background temperature is derived from results of geothermal modeling of Vrancea lithosphere (Demetrescu and Andreescu, 1994) (Fig. 3).

Viscosity is an important physical parameter in stress modeling because it influences the stress state and results in strengthening or weakening of Earth's material. Though it is the least-known physical parameter of the model, the viscosity of the Vrancea slab can be constrained by observations of the regional strain rates.

Table 1
Laterally averaged compressional seismic wave velocities (v_p), density (ρ_*) calculated from v_p, and average temperature (T_*)

Depth (km)	v_p (km s^{-1})[a]	ρ_* (10^3 kg m^{-3})[b]	T_* (°C)[c]
0	2.7	1.59	20
2.5	3.5	1.84	80
5.0	4.5	2.17	130
7.5	5.2	2.39	180
10.0	5.7	2.55	230
12.5	5.8	2.58	290
15.0	5.9	2.61	350
20.0	6.2	2.71	420
25.0	6.7	2.87	510
30.0	6.9	2.94	600
35.0	7.0	2.97	670
40.0	8.0	3.28	740
50.0	8.1	3.32	820

[a] Hauser et al. (2001, 2002).
[b] Krasovsky (1989).
[c] Demetrescu and Andreescu (1994).

Intermediate-depth earthquakes in the Vrancea region provide an indirect measure of the rate of strain release within the seismogenic body (8×10^8 N m year^{-1}, Wenzel et al., 1999; Ismail-Zadeh et al., 2000). Therefore, the strain rate (ratio between stress and viscosity), as a result of the Vrancea earthquakes, is estimated to be 7.5×10^{-15} s^{-1} (Wenzel et al., 1999; the estimation is based on Kostrov's (1974) formula). This strain rate was used as a constraint on the viscosity of the model slab in our test computations of the flow (and strain rate) for various viscosity ratios between slab and mantle. Based on these tests, we adopted the background viscosity $\mu_*(\mathbf{x})$ to be 10^{22} Pa s for the Vrancea slab, 10^{23} Pa s for the crust, and 10^{20} Pa s for the mantle. The model parameters are summarized in Table 2.

We consider free-slip conditions at the upper and lower boundaries of the model domain and symmetry conditions at the side (vertical) boundaries. To avoid an effect of the lateral boundary conditions on the numerical results, we extended the modeled domain in horizontal directions by a factor of two. The effect of the surface loading due to the Carpathian Mountains is not considered, because this loading would have insignificant influence on the stress in the slab (as was shown in two-dimensional models of the Vrancea slab evolution; Ismail-Zadeh et al., 2004). According to geodynamic models of the region (e.g., Sperner et al., 2001), the Vrancea slab is at its late evolutionary stage and sinks into the mantle solely under the influence of gravity. Hence, neither horizontal nor vertical velocities are superimposed on the model domain, and flow and induced tectonic stresses are considered to be due to buoyancy forces alone.

Table 2
Model parameters

Background crustal density	Fig. 3 and Table 1
Background mantle density	Fig. 3
Background crustal viscosity (Pa s)	10^{23}
Background mantle viscosity (Pa s)	10^{20}
Background slab viscosity (Pa s)	10^{22}
Background temperature	Fig. 3
Coefficient of thermal expansion, α (K^{-1})	3×10^{-5}
Activation energy, E (J mol^{-1})	5×10^5
Activation volume, V (m^3 mol^{-1})	2×10^{-5}
Universal gas constant, R (J mol^{-1} K^{-1})	8.3
Acceleration due to gravity, g (m s^{-2})	9.8
Vertical size of the model, l_3 (km)	350
Horizontal sizes of the model, l_1 and l_2 (km)	1050
Stress scale (MPa)	4×10^4

The numerical solution to the problem is based on the introduction of a two-component vector velocity potential (replacing the three components of vector velocity in Eqs. (1) and (2)) and on the application of the Eulerian finite-element method with a tricubic-spline basis for computing the vector potential (Ismail-Zadeh et al., 2001). The tensor of tectonic stress σ_{ij} is then computed using the relationship $\sigma_{ij} = \mu(T, P)e_{ij}$.

The numerical models, with a spatial resolution of 10 km × 10 km × 5 km, were run on an IBM SP2 parallel computer. The accuracy of the solutions has been verified by several tests, including numerical grid changes and total mass changes (Ismail-Zadeh et al., 2001) and comparison with the simple analytical solution to the 3D Stokes equation combined with the advection of density equation (Trushkov, 2002).

5.2. Predicted crustal and mantle flow

Fig. 6 presents the 3D pattern of flow predicted by the model. The main feature is that the gravitational sinking of the slab beneath the Vrancea region induces downwelling (blue cones) and associated upwelling (orange cones) in the mantle. In fact, the 3D flow is rather complicated at the depths of the intermediate-depth seismicity: toroidal (in horizontal planes) flow at depths between about 100 and 200 km coexists with poloidal (in vertical planes) flow. The horizontal flow at the bottom of the model is related to the prescribed boundary conditions and is an artifact. This shortcoming is associated with the fact that the slab can be seen in seismic tomographic images to depths of 350 km, and we have no information on either the presence or absence of the high-velocity anomaly deeper in the mantle. Hence, to avoid the ambiguity with the length of the slab in the modeling and keeping in mind that our aim is to evaluate flow and stress in the region at depths between 70 and 220 km where large earthquakes occur, we adopted the depth of the model domain to be 350 km.

The modeled vertical movements in the crust are shown in Fig. 7 (horizontal slice at depth of 15 km). The areas of major uplift in the model coincide with the East Carpathian and Dobrogea orogens and surround the Transylvanian basin. These model findings are corroborated by the results from fission track

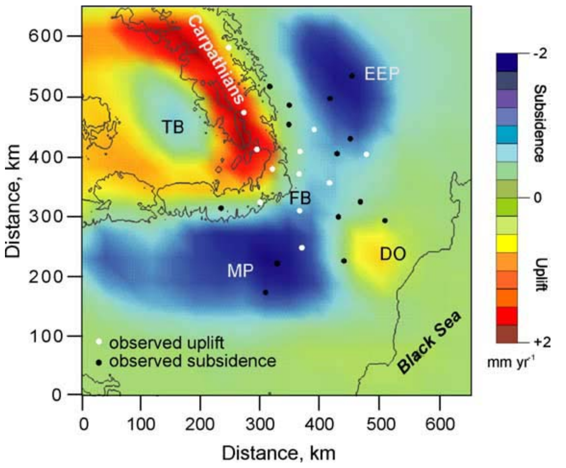

Fig. 7. Map of predicted uplift and subsidence in the SE-Carpathians at 15 km depth. White and black dots illustrate the relative vertical movements at the surface as derived from GPS measurements (Dinter et al., 2001). Isolines present the surface topography. DO, Dobrogea orogen; EEP, Eastern European platform; FB, Foscani basin; MP, Moesian platform; and TB, Transylvanian basin.

analysis in the eastern Carpathian region and Transylvanian basin that demonstrate uplift of several hundred meters since at least Pliocene times (Sanders et al., 1999, 2002). The Focsani basin is situated between the predicted areas of uplift and subsidence. The modeled crustal movements beneath the basin are directed downward and consistent with the analysis of recent vertical movements in the Foscani basin (Tarapoanca et al., 2003). The areas of modeled subsidence correlate with the Moesian and East European platforms. This result is confirmed by the observed tectonic subsidence of the external Carpathian–Moesian platform based on the backstripping analysis (Matenco et al., 2003). The numerical results on vertical crustal movements in the SE-Carpathians agree with the results of geomorphological, geodetic, and geological analysis of recent crustal movements in the region (Radulescu et al., 1996; Zugravescu et al., 1998).

We want to emphasize that the pattern of vertical crustal movements should be considered in a qualitative way (while the results are quantitative) for the

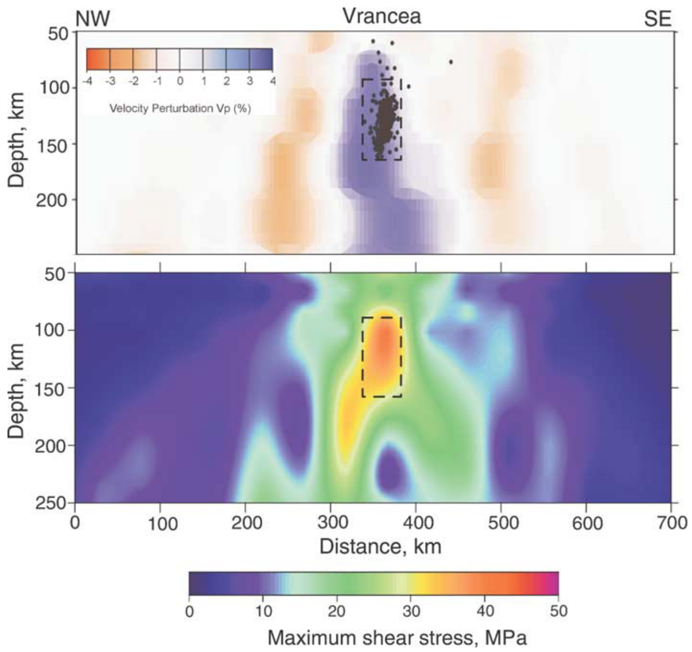

Fig. 8. Comparison of the location of positive P-wave velocity anomalies, earthquake hypocenters, and predicted maximum shear stress. Upper panel: NW–SE seismic tomography cross-section through the SE-Carpathian region (after Martin et al., 2001) and the projection onto this cross-section of the hypocenters of the Vrancea earthquakes from the last decade. Lower panel: predicted maximum shear stress for the same cross-section. The dashed boxes delineate the area of hypocenters and maximum shear stress.

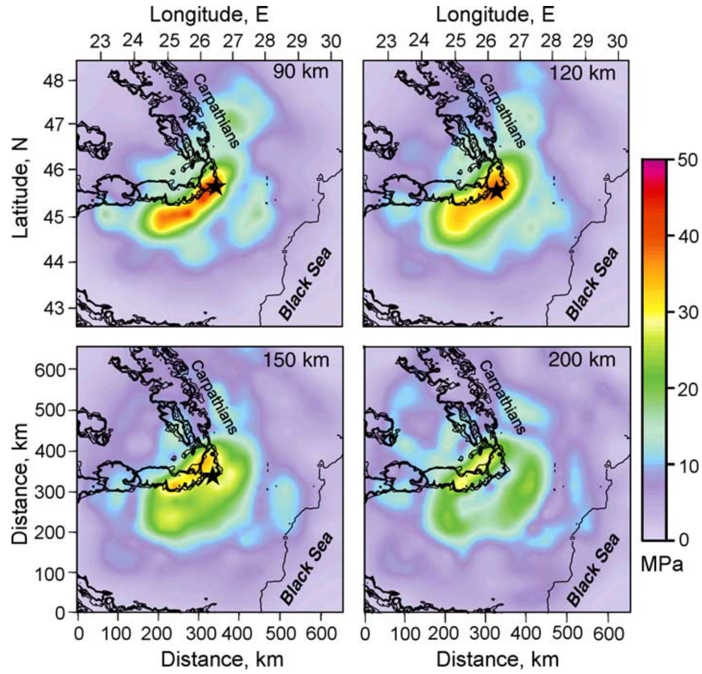

Fig. 9. Maximum shear stress beneath the SE-Carpathians at different mantle depths. Isolines present the surface topography. Star marks the location of the Vrancea intermediate-depth earthquakes.

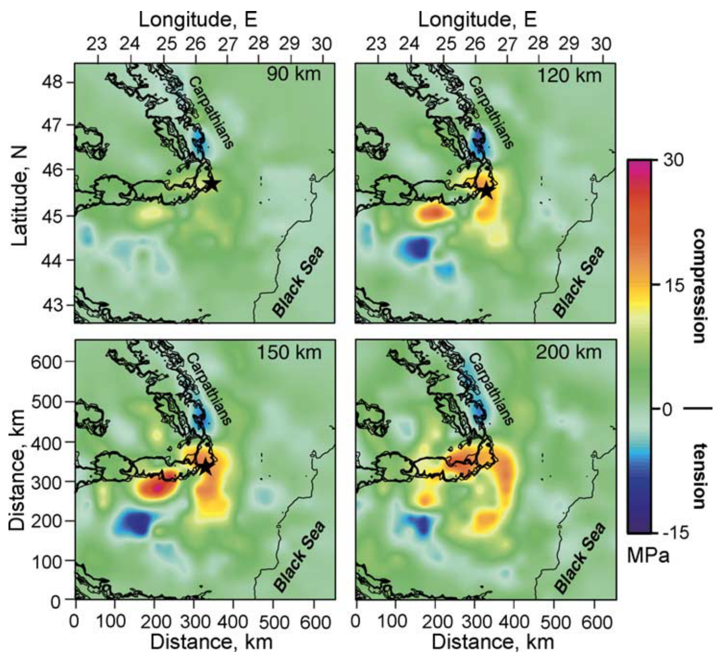

Fig. 10. Maximum horizontal stress (compression is positive and tension is negative) beneath the SE-Carpathians at different mantle depths. Isolines present the surface topography. Star marks the location of the Vrancea intermediate-depth earthquakes.

following reasons. First, knowledge of the physical properties (density, effective viscosity, temperature) of the crust in the SE-Carpathians is still poor, despite the existence of the seismic crustal models based on the two refraction profiles and results of regional geological and geothermal studies. Second, we do not know much about the rheology of the lower crust, which may influence the vertical movements of the upper crust (Andreescu and Demetrescu, 2001; Lenkey et al., 2002). Third, the reported GPS rates of vertical movements in the region (Dinter et al., 2001) were overestimated (G. Dinter, 2003, personal communication). Ongoing GPS campaigns will probably provide better constraints on the vertical movements in the SE-Carpathian region in the near future. Fourth, the comparison of short-term GPS rates of surface movements with the predicted long-term movements due to mantle dynamics should be done very carefully in *seismically active* regions. The crustal deformation in such regions is comprised of both post-seismic and tectonic deformation, which should be taken into consideration in a quantitative comparison.

5.3. Predicted tectonic stress

To examine whether the predicted areas of stress localization are consistent with the areas of intermediate-depth seismicity in the region, we compare the predicted zones of maximum shear stress localization with the hypocenters of intermediate-depth earthquakes. The maximum shear stress (see Appendix A for the stress calculation) on the NW–SE cross-section through the Vrancea region is presented in Fig. 8. The stress is localized in a narrow zone that coincides with the projection of earthquake hypocenters onto the same cross-section. The calculated maximum shear stress is also shown in horizontal planes at depths of 90, 120, 150, and 200 km in Fig. 9. The predicted maximum shear stress is associated with the descending Vrancea slab (cold lithospheric body), localized at depths of about 80–180 km, diminishes to the depth of 220 km, and encompasses the area of major Vrancea intermediate-depth events.

The stress concentration in the Vrancea slab during a period between two large earthquakes could have some important implications for the location of a future rupture. Chinnery (1963) showed that shear stresses rise in an area much wider than just in the area of fault tips. The importance of the Chinnery's discovery was realized later, when lobes of off-fault aftershocks were seen to be associated with calculated increases in shear or Coulomb failure stress (Stein, 1999, and references therein).

Also we estimate the maximum horizontal stress (see Appendix A for the stress calculation) in the modeled region (Fig. 10). The horizontal compression is localized in the areas of large earthquakes. Using numerous fault-plane solutions for intermediate-depth events, Oncescu and Trifu (1987) showed that the axes of compressional stress are almost horizontal (see Fig. 2). The model results indicate also high stresses in the aseismic southwestern portion of the slab beneath the Moesian platform. The complex geometry of the zone of maximum compressional stress reflects the pattern of flow induced by the Vrancea slab sinking in the mantle under the influence of gravity.

6. Discussion

We have modeled tectonic stresses induced by the descending high-velocity body (interpreted as a relic lithospheric slab) beneath the SE-Carpathians (Vrancea earthquake-prone region) and shown that the seismic events at intermediate depths are associated with the zones of maximum shear stress localization. Horizontal compression at these depths agrees well with the stress determination based on the focal mechanisms of the intermediate-depth earthquakes. Small-scale discrepancies between the model predictions and regional observations can be attributed to the model limitations and uncertainties discussed below.

An interpretation of absolute values of lateral heterogeneities in seismic wave velocities has uncertainties regarding thermal anomaly or differences in chemical composition. Moreover, a refined model of P-wave seismic tomography that considers crustal structure can improve the current model at uppermost mantle depths. Another source of uncertainty comes from the choice of mantle and slab compositions in the modeling of mantle temperature from the P-wave seismic velocities. Unfortunately, there are no data on the composition of the mantle beneath the SE-Carpathians, except a few petrological studies of igneous rocks from the Neogene eastern Carpathian volcanic zone (Nitoi et al., 2002, and references therein).

As direct temperature measurements are limited to depths of a few kilometers from the surface, the information on the average temperature versus depth comes from geothermal conductivity modeling (Demetrescu and Andreescu, 1994). Additional information from geothermobarometry of xenoliths may better constrain the background temperature profiles (Sobolev et al., 1996).

Viscosity in the mantle beneath the Vrancea region might be influenced by the presence of water at 50–100 km depth. In the modeling, we used a temperature- and pressure-dependent viscosity for the mantle and did not take into account the dependence of viscosity on water. Mei et al. (2002) showed that, due to the combined effects of water and melt weakening, the mantle viscosity in subduction zones can vary by three orders of magnitude over the depth-range 60–120 km. The stress-dependent viscous rheology (power-law creep) and low-temperature plasticity (the Peierls mechanism; Kameyama et al., 1999) may also influence the magnitude of the tectonic stress in the Vrancea lithospheric slab.

Despite the model limitations, we have demonstrated the causal relationship between tectonic stress and seismic activity in the region as a consequence of viscous flow induced by the Vrancea slab descending into the mantle under the influence of gravity. Moreover, we have shown that our model, with relatively few adjustable parameters, can provide a sound interpretation of the observed seismic data.

In addition to viscous stress induced by the descending Vrancea slab, other processes might contribute to the stress generation. An increase of shear stress due to the descending slab is one of the possibilities analyzed here. Another process could be a plastic instability at high temperature, when runaway shear slip (failure) occurs at even relatively low shear stresses (Griggs and Baker, 1969). Faulting due to metamorphic phase transitions (Green and Burnley, 1989) or dehydration-induced embrittlement (Raleigh and Paterson, 1965; Hacker et al., 2003) may also play a role in the regional stress generation and release. However, estimations of the cumulative annual seismic moment observed and associated with the volume change due to the basalt-eclogite phase changes in the Vrancea slab show that a pure phase-transition model cannot solely explain the intermediate-depth earthquakes in the region (Ismail-Zadeh et al., 2000).

The question that remains is why earthquakes are located only in a part of the maximum shear stress zone (see Fig. 9). Ismail-Zadeh (2003) attempted to answer this question by making use of a simple analytical model for corner flow (Batchelor, 1967). He demonstrated that the pattern of tectonic stress, induced by a descending slab in subduction zones, differs from that in zones of collision. Maximum shear stress migrates from the upper surface of the descending slab to its lower surface due to changes in dynamics of the descending slab (from slab subduction due to applied lateral forces to slab retreat due to gravity forces). Moreover, as shown in the block-and-fault model of the Vrancea region (Ismail-Zadeh et al., 1999; Soloviev and Ismail-Zadeh, 2003), large earthquakes are likely to occur at the lower surface of the descending slab rather than at its upper surface.

Intermediate-depth earthquakes observed in several places in the world (Pamir-Hindu Kush, the Mediterranean region, Caucasus, Zagros, and Assam) are associated with plate collisions. However, due to the lack of tomography studies, the distribution of earthquake hypocenters with respect to the descending slab beneath these regions is not as well constrained as in the Vrancea region. High-resolution seismic tomography in the regions of intermediate-depth seismicity is crucial (i) to answer the question about *hypocenter locations with respect to the descending slab* and (ii) to clarify *the role of buoyancy forces in contemporary stress generation, its localization and association with seismic events*.

7. Conclusion

Based on data from seismic tomography, seismic refraction profiles, heat flow and on the knowledge of geodynamic evolution of the region, we have performed a quantitative analysis of contemporary slow mantle flow and tectonic stress beneath the SE-Carpathians. We have demonstrated a correlation between the location of intermediate-depth earthquakes and the predicted localizations of maximum shear stress and horizontal compression. Therefore, the buoyancy forces, which result from realistic temperature and density distributions in the crust and mantle, can govern the present deformation beneath the SE-Carpathians and explain the regional stress pattern and intermediate-depth seismicity. Refined seismic tomography results and geothermal modeling will improve the present tectonic stress model.

Acknowledgements

We are very grateful to M. Martin for providing the data on seismic tomography, M. Andreescu and C. Demetrescu for the regional crustal temperature models and fruitful discussions on the geothermal evolution of the region, to K. Bonjer, J. Dirkzwager, K. Fuchs, R. Hackney, F. Hauser, S. Karato, J. Ritter, B. Sperner, I. Tsepelev, and F. Wenzel for useful discussions on the regional seismicity and geodynamics, gravity, temperature, and numerical modeling and critical comments on initial versions of the manuscript. We thank A. Wüstefeld for his assistance in digital data preparation and drawing several figures. Constructive reviews and suggestions by D. Yuen and anonymous reviewer and editorial comments by P. van Keken are acknowledged. This publication was supported by the Alexander von Humboldt Foundation, Program of the Russian Academy of Sciences "Deep Structure of the Earth", Collaborative Research Centre SFB 461 "Strong Earthquakes", and National Science Foundation (EAR 0105945).

Appendix A. Calculation of principal stress, maximum shear stress, and maximum horizontal stress from the deviatoric stress tensor

The principal stresses $\sigma_1 \geq \sigma_2 \geq \sigma_3$ are the roots of the cubic equation (e.g., Jaeger and Cook, 1984)

$$\sigma^3 - I_1\sigma^2 - I_2\sigma - I_3 = 0,$$

where I_k ($k=1, 2, 3$) are three invariants of the deviatoric (tectonic) stress tensor:

$$I_1 = \tau_{11} + \tau_{22} + \tau_{33},$$

$$I_2 = -(\tau_{11}\tau_{22} + \tau_{11}\tau_{33} + \tau_{22}\tau_{33}) + \tau_{12}^2 + \tau_{13}^2 + \tau_{23}^2,$$

$$I_3 = \tau_{11}\tau_{22}\tau_{33} + 2\tau_{12}\tau_{13}\tau_{23} - \tau_{11}\tau_{23}^2 - \tau_{22}\tau_{13}^2 - \tau_{33}\tau_{12}^2.$$

Using Cardano's formula (Kurosh, 1972), we find an analytical expression for the principal stresses from the cubic equation:

$$\sigma_{1,2,3} = \left[-\frac{q}{2} + \left(\frac{q^2}{4} + \frac{p^3}{27}\right)^{1/2}\right]^{1/3} + \left[-\frac{q}{2} - \left(\frac{q^2}{4} + \frac{p^3}{27}\right)^{1/2}\right]^{1/3},$$

where

$$p = -\frac{1}{3}I_1^2 - I_2, \qquad q = -\frac{2}{27}I_1^3 - \frac{1}{3}I_1 I_2 - I_3.$$

The maximum shear stress $\tau_{\max}$ is calculated from the principal stresses:

$$\tau_{\max} = 0.5(\sigma_1 - \sigma_3)$$

The maximum horizontal stress S_{H} is calculated from the tensor of tectonic stress τ_{ij} as

$$S_H = \max(\theta_{13}, \theta_{23})$$

where

$$\theta_{13} = \tau_{23}\sin\alpha + \tau_{13}\cos\alpha$$

$$\theta_{23} = \tau_{23}\cos\alpha - \tau_{13}\sin\alpha$$

and

$$\alpha = 0.5\arctan\frac{2\tau_{12}}{\tau_{11} - \tau_{22}}.$$

References

Agee, C.B., 1993. Petrology of the mantle transition zone. Ann. Rev. Earth Planet. Sci. 21, 19–41.

Aki, K., Christofferson, A., Husebye, E.S., 1977. Determination of the three dimensional seismic structure of the lithosphere. J. Geophys. Res. 82, 277–296.

Andreescu, M., Demetrescu, C., 2001. Rheological implications of the thermal structure of the lithosphere in the convergence zone of the eastern Carpathians. J. Geodyn. 31, 373–391.

Bass, J.D., 1995. Elasticity of minerals, glasses, and melts. In: Ahrens, T.J. (Ed.), Mineral Physics and Crystallography, A Handbook of Physical Constants. American Geophysical Union, pp. 45–63.

Batchelor, G.K., 1967. An Introduction to Fluid Dynamics. Cambridge University Press, Cambridge, 615 pp.

Bijwaard, H., Spakman, W., 2000. Non-linear global P-wave tomography by iterated linearized inversion. Geophys. J. Int. 141, 71–82.

Chinnery, M.A., 1963. The stress changes that accompany strike-slip faulting. Bull. Seismol. Soc. Am. 53, 921–932.

Csontos, L., Nagymarosy, A., Horvath, F., Kovac, M., 1992. Tertiary evolution of the intra-Carpathian area; a model. Tectonophysics 208, 221–241.

Demetrescu, C., Andreescu, M., 1994. On the thermal regime of some tectonic units in a continental collision environment in Romania. Tectonophysics 230, 265–276.

Demetrescu, C., Nielsen, S.B., Ene, M., Serban, D.Z., Polonic, G., Andreescu, M., Pop, A., Balling, N., 2001. Lithosphere thermal structure and evolution of the Transylvanian depression – insight from new geothermal measurements and modelling results. Phys. Earth Planet. Int. 126, 249–267.

Dinter, G., Nutto, M., Schmitt, G., Schmidt, U., Ghitau, D., Marcu, C., 2001. Three dimensional deformation analysis with respect to plate kinematics in Romania. Reports Geodesy 2, 29–42.

Dziewonski, A.M., Anderson, D.L., 1981. Preliminary Reference Earth Model (PREM). Phys. Earth Planet. Int. 25, 297–356.

Evans, J.R., Achauer, U., 1993. Teleseismic velocity tomography using the ACH-method: theory and application to continental-scale studies. In: Iyer, K.M., Hirahara, K. (Eds.), Seismic Tomography; Theory and Practice. Chapman and Hall, London, pp. 319–360.

Forte, A.M., Woodward, R.L., Dziewonski, A.M., 1994. Joint inversions of seismic and geodynamic data for models of three-dimensional mantle heterogeneity. J. Geophys. Res. 99 (21), 857–21, 887.

Forte, A.M., Dziewonski, A.M., O'Connell, R.J., 1995. Thermal and chemical heterogeneity in the mantle: a seismic and geodynamic study of continental roots. Phys. Earth Planet. Int. 92, 45–55.

Fuchs, K., Bonjer, K., Bock, G., Cornea, I., Radu, C., Enescu, D., Jianu, D., Nourescu, A., Merkler, G., Moldoveanu, T., Tudorache, G., 1977. The Romanian earthquake of March 4, 1977. II. Aftershocks and migration of seismic activity. Tectonophysics 53, 225–247.

Girbacea, R., Frisch, W., 1998. Slab in the wrong place: lower lithospheric mantle delamination in the last stage of the eastern Carpathian subduction retreat. Geology 26 (7), 611–614.

Goes, S., Govers, R., Vacher, P., 2000. Shallow mantle temperatures under Europe from P and S wave tomography. J. Geophys. Res. 105 (11), 153–169.

Green, D.H., Falloon, T.J., 1998. Pyrolite: a Ringwood concept and its current expression. In: Jackson, I. (Ed.), The Earth's Mantle. Cambridge University Press, Cambridge, pp. 311–378.

Green II, H.W., Burnley, P.C., 1989. A new self-organizing mechanism for deep-focus earthquakes. Nature 341, 733–737.

Griffin, W.L., O'Reilly, S.Y., Ryan, C.G., Gaul, O., Ionov, D.A., 1998. Secular variation in the composition of subcontinental lithospheric mantle: geophysical and geodynamic implications. In: Braun, J., et al. (Eds.), Structure and Evolution of the Australian Continent, vol. 26. American Geophysical Union, Geodynamics Series, pp. 1–26.

Griggs, D.T., Baker, D.W., 1969. The origin of deep-focus earthquakes. In: Mark, H., Fernbach, S. (Eds.), Properties of Matter Under Unusual Conditions. Wiley, New York, pp. 23–42.

Gutenberg, B., Richter, C.F., 1954. Seismicity of the Earth and Associated Phenomena, second ed. Princeton University Press, Princeton, NJ, 310 pp.

Hacker, B.R., Peacock, S.M., Abers, G.A., Holloway, S.D., 2003. Subduction factory. 2. Are intermediate-depth earthquakes in subducting slabs linked to metamorphic dehydration reactions? J. Geophys. Res. 108, 2030, doi:10.1029/2001JB001129.

Hackney, R., Martin, M., Ismail-Zadeh, A., Sperner, B., Ioane, D., CALIXTO Working Group, 2002. The gravity effect of the subducted slab beneath the Vrancea region, Romania. In: Michalik, J., Simon, L., Vozar, J. (Eds.), Proceedings of the XVIIth Congress of the Carpathian-Balkan Geological Association, vol. 53. Bratislava, September 1–4, 2002, Geologica Carpathica, pp. 119–121.

Hammond, W.C., Humphreys, E.D., 2000a. Upper mantle seismic wave velocity: effects of realistic partial melt geometries. J. Geophys. Res. 105 (10), 10,975–10,986.

Hammond, W.C., Humphreys, E.D., 2000b. Upper mantle seismic wave velocity: effects of realistic partial melt distribution. J. Geophys. Res. 105 (10), 10,987–10,999.

Hauser, F., Raileanu, V., Fielitz, W., Bala, A., Prodehl, C., Polonic, G., Schulze, A., 2001. VRANCEA99 – the crustal structure beneath the southeastern Carpathians and the Moesian Platform from a seismic refraction profile in Romania. Tectonophysics 340, 233–256.

Hauser, F., Prodehl, C., Landes, M., VRANCEA Working Group, 2002. Seismic experiments target earthquake-prone region in Romania. EOS 83 (41), 457, 462–463.

Hettel, S., Regenauer-Lieb, K., Sperner, B., Wenzel, F., 2000. Last signal of a fading slab: Data, constraints, and FE-modelling of Vrancea (SE-Romania). EOS, Transactions of the American Geophysical Union 81 (48), F1090.

Ioane, D., Atanasiu, L., 1998. Gravimetric geoids and geophysical significances in Romania. In: Ioane, D. (Ed.), Monograph of Southern Carpathians, Reports on Geodesy, vol. 7. Institute of Geodesy, Geodetic Astronomy, Warsaw University of Technology, Warsaw, Poland, pp. 157–175.

Ismail-Zadeh, A.T., 2003. Modelling of stress and seismicity in the south-eastern Carpathians: basis for seismic risk estimation. In: Beer, T., Ismail-Zadeh, A.T. (Eds.), Risk Science and Sustainability. Kluwer Academic Publishers, Dordrecht, pp. 149–162.

Ismail-Zadeh, A.T., Keilis-Borok, V.I., Soloviev, A.A., 1999. Numerical modelling of earthquake flows in the southeastern Carpathians (Vrancea): effect of a sinking slab. Phys. Earth Planet. Int. 111, 267–274.

Ismail-Zadeh, A.T., Panza, G.F., Naimark, B.M., 2000. Stress in the descending relic slab beneath the Vrancea region, Romania. Pure Appl. Geophys. 157, 111–130.

Ismail-Zadeh, A.T., Korotkii, A.I., Naimark, B.M., Tsepelev, I.A., 2001. Numerical modelling of three-dimensional viscous flow under gravity and thermal effects. Comput. Math. Math. Phys. 41 (9), 1331–1345.

Ismail-Zadeh, A., Mueller, B., Wenzel, F., 2004. Modelling of descending slab evolution beneath the SE-Carpathians: implications for seismicity. In: Wenzel, F. (Ed.), Perspectives in Modern Seismology, Lecture Notes in Earth Sciences, vol. 105. Springer-Verlag, Heidelberg, pp. 205–226.

Jaeger, J.C., Cook, N.G.W., 1984. Fundamentals of Rock Mechanics, third ed. Chapman and Hall, London, New York, 593 pp.

Jiricek, R., 1979. Tectonic development of the Carpathian arc in the Oligocene and Neogene. In: Mahel, M. (Ed.), Tectonic Profiles Through the Western Carpathians. Geol. Inst. Dionyz Stur, pp. 205–214.

Jordan, T.H., 1979. Mineralogies, densities and seismic velocities of garnet lherzolites and their geophysical implications. In: Boyd, F.R., Meyer, H.O.A. (Eds.), The Mantle Sample: Inclusions in Kimberlites and Other Volcanics. American Geophysical Union, Washington, DC, pp. 1–14.

Kameyama, M., Yuen, D.A., Karato, S.-I., 1999. Thermal-mechanical effects of low-temperature plasticity (the Peierls mechanism) on the deformation of a viscoelastic shear zone. Earth Planet. Sci. Lett. 168, 159–172.

Karato, S.-I., 1993. Importance of anelasticity in the interpretation of seismic tomography. Geophys. Res. Lett. 20, 1623–1626.

Karato, S.-I., 2004. Mapping water content in the upper mantle. In: Eiler, J. (Ed.). Inside the Subduction Factory. Geophysical Monographs Series, vol. 138. American Geophysical Union, Washington, DC, pp. 163–180.

Kostrov, V.V., 1974. Seismic moment and energy of earthquakes, and seismic flow of rocks. Izv. AN SSSR/Earth Phys. 1, 13–20.

Krasovsky, S.S., 1989. Gravity Modeling of Deep-Seated Crustal Features and Isostasy. Naukova Dumka, Kiev, 268 pp. (in Russian).

Kurosh, A.G., 1972. Higher Algebra. Mir Publishers, Moscow, p. 428.

Lenkey, L., Dovenyi, P., Horvath, F., Cloetingh, S.A.P.L., 2002. Geothermics of the Pannonian basin and its bearing on the neotectonics. In: Cloetingh, S.A.P.L., et al. (Eds.), Neotectonics and Surface Processes: The Pannonian Basin and Alpine/Carpathian System, vol. 3. EGU Stephan Mueller Special Publication Series, pp. 29–40.

Linzer, H.-G., 1996. Kinematics of retreating subduction along the Carpathian arc, Romania. Geology 24, 167–170.

Martin, M., Achauer, U., Kissling, E., Mocanu, V., Musacchio, G., Radulian, M., Wenzel, F., CALIXTO Working Group, 2001. First results from the tomographic experiment CALIXTO'99 in Romania. Geophys. Res. Abst. 3, SE1.02.

Martin, M., CALIXTO Working Group, 2003. High resolution teleseismic P-wave tomography for SE-Romania. Geophys. Res. Abst. 5, 10512.

Matenco, L., Bertotti, G., Cloetingh, S., Dinu, C., 2003. Subsidence analysis and tectonic evolution of the external Carpathian–Moesian platform region during Neogene times. Sedim. Geol. 156, 71–94.

McKenzie, D.P., 1972. Active tectonics of the Mediterranean region. Geophys. J. R. Astron. Soc. 30, 109–185.

Mei, S., Bai, W., Hiraga, T., Kohlstedt, D.L., 2002. Influence of melt on the creep behavior of olivine–basalt aggregates under hydrous conditions. Earth Planet. Sci. Lett. 201, 491–507.

Nitoi, E., Munteanu, M., Marincea, S., Paraschivoiu, V., 2002. Magma-enclave interactions in the East Carpathian subvolcanic zone, Romania: petrogenetic implications. J. Volcan. Geother. Res. 118, 229–259.

Niu, Y., 1997. Mantle melting and melt extraction processes beneath ocean ridges: evidence from abyssal peridotites. J. Petrol. 38, 1047–1074.

Oncescu, M.C., 1984. Deep structure of the Vrancea region, Romania, inferred from simultaneous inversion for hypocentres and 3-D velocity structure. Ann. Geophys. 2, 23–28.

Oncescu, M.C., Bonjer, K.P., 1997. A note on the depth recurrence and strain release of large Vrancea earthquakes. Tectonophysics 272, 291–302.

Oncescu, M.C., Trifu, C.I., 1987. Depth variation of moment tensor principal axes in Vrancea (Romania) seismic region. Ann. Geophys. 5, 149–154.

Pana, D., Erdmer, P., 1996. Kinematics of retreating subduction along the Carpathian arc, Romania: comment. Geology 24, 862–863.

Pana, D., Morris, G.A., 1999. Slab in the wrong place: lower lithospheric mantle delamination in the last stage of the eastern Carpathian subduction retreat: comment. Geology 27, 665–666.

Radu, C., 1979. Catalogue of strong earthquakes occurred on the Romanian territory. Part I – before 1901; Part II – 1901–1979. In: Cornea, I., Radu, C. (Eds.), Seismological Studies on the March 4, 1977, Earthquake, Bucharest, Romanian, pp. 723–752 (in Romanian).

Radu, C., 1991. Strong earthquakes occurred on the Romanian territory in the period 1901–1990. Vitralii 3, 12–13 (in Romanian).

Radulescu, F., Mocanu, V., Nacu, V., Diaconescu, C., 1996. Study of recent crustal movements in Romania: a review. J. Geodyn. 22, 33–50.

Raleigh, C.B., Paterson, M.S., 1965. Experimental deformation of serpentine and its tectonic consequences. J. Geophys. Res. 70, 3965–3985.

Sanders, C.A.E., Andriessen, P.A.M., Cloetingh, S.A.P.L., 1999. Life cycle of the East Carpathian orogen: erosion history of a doubly vergent critical wedge assessed by fission track thermochronology. J. Geophys. Res. 104 (29), 095–29, 112.

Sanders, C., Huismans, R., van Wees, J.D., Andriessen, P., 2002. The Neogene history of the Transylvanian basin in relation to its surrounding mountains. In: Cloetingh, S.A.P.L., et al. (Eds.), Neotectonics and Surface Processes: The Pannonian Basin and Alpine/Carpathian System, vol. 3. EGU Stephan Mueller Special Publication Series, pp. 121–133.

Schmidt, S., Götze, H.-J., 1998. Interactive visualization and modification of 3D-models using GIS-functions. Phys. Chem. Earth 23 (3), 289–295.

Sobolev, S.V., Zeyen, H., Stoll, G., Werling, F., Altherr, R., Fuchs, K., 1996. Upper mantle temperatures from teleseismic tomography of French Massif Central including effects of composition, mineral reactions, anharmonicity, anelasticity and partial melt. Earth Planet. Sci. Lett. 139, 147–163.

Soloviev, A.A., Ismail-Zadeh, A.T., 2003. Models of dynamics of block-and-fault systems. In: Keilis-Borok, V.I., Soloviev, A.A. (Eds.), Nonlinear Dynamics of the Lithosphere and Earthquake Prediction. Springer-Verlag, Heidelberg, pp. 69–138.

Sperner, B., CRC 461 Team, 2004. Monitoring of slab detachment in the SE-Carpathians. In: Wenzel, F. (Ed.), Perspectives in Modern

Seismology, Lecture Notes in Earth Sciences, vol. 105. Springer-Verlag, Heidelberg, pp. 189–204.

Sperner, B., Lorenz, F., Bonjer, K., Hettel, S., Müller, B., Wenzel, F., 2001. Slab break-off – abrupt cut or gradual detachment? New insights from the Vrancea region (SE Carpathians, Romania). Terra Nova 13, 172–179.

Smith, G.P., Wiens, D.A., Fischer, K.M., Dorman, L.M., Webb, S.C., Hildebrand, J.A., 2001. A complex pattern of mantle flow in the Lau backarc. Science 292, 713–716.

Stein, R., 1999. The role of stress transfer in earthquake occurrence. Nature 402, 605–609.

Takei, Y., 2000. Acoustic properties of partially molten media studied on a simple binary system with a controllable dihedral angle. J. Geophys. Res. 105, 16,665–16,682.

Tarapoanca, M., Bertotti, G., Matenco, L., Dinu, C., Cloetingh, S.A.P.L., 2003. Architecture of the Focsani depression: a 13 km deep basin in the Carpathians bend zone (Romania). Tectonics 22 (6), 1074, doi:10.1029/2002TC001486.

Trushkov, V.V., 2002. An example of (3 + 1)-dimensional integrable system. Acta Appl. Math. 72 (1–2), 111–122.

Wenzel, F., Lorenz, F.P., Sperner, B., Oncescu, M.C., 1999. Seismotectonics of the Romanian Vrancea area. In: Wenzel, F., Lungu, D., Novak, O. (Eds.), Vrancea Earthquakes: Tectonics, Hazard and Risk Mitigation. Kluwer Publishers, Dordrecht, pp. 15–25.

Wortel, M.J.R., Spakman, W., 2000. Subduction and slab detachment in the Mediterranean-Carpathian region. Science 290, 1910–1917.

Zugravescu, D., Polonic, G., Horomnea, M., Dragomir, V., 1998. Recent vertical crustal movements on the Romanian territory, major tectonic compartments and their relative dynamics. Rev. Roum. Geophys. 42, 3–14.

Buoyancy-Driven Deformations and Contemporary Tectonic Stress in the Lithosphere beneath North-Central Italy

A. Aoudia, A. T. Ismail-Zadeh and G. F. Panza

Abstract. On the basis of a revisited crust and uppermost mantle Earth structure that supports delamination processes beneath North-Central Italy we study the continental deformation and model the contemporary flow and stress distribution in the lithosphere. The rate of the modeled lithospheric flow is in agreement with GPS data and its patterns explain the heat flux, the regional geology and provide a new background for the genesis and age of the recent Tuscan magmatism. The modeled stress in the lithosphere is spatially correlated with gravitational potential energy patterns and show that internal buoyancy forces, solely, can explain the coexisting regional contraction and extension and the unusual intermediate depth seismicity.

Introduction

The juxtaposed contraction and extension observed in the crust of the North-Central Italian Apennines (Fig. 1) and elsewhere has, for a long time, attracted the attention of geoscientists and is a long-standing enigmatic feature. Several models, invoking mainly external forces, have been put forward to explain the close association of these two end-member deformation mechanisms clearly observed by seismological and geological investigations [*e.g. Frepoli and Amato, 1997; Montone et al., 1999*; *Doglioni et al., 1999*]. These models appeal to interactions along plate margins or at the base of the lithosphere, or to subduction processes [*e.g. Negredo et al., 1999; Wortel and Spakman, 2000*]. Some of the geodynamic models were constrained by earth models that resolve fairly well either the crust [*e.g. Pialli et al., 1998*] or the mantle structures [*e.g. Wortel and Spakman, 2000*] but not the crust-uppermost mantle structures [*e.g. Agostinetti et al., 2002; Chimera et al., 2003*].

The geodynamic complexity of the Central part of Italy makes the kinematics of the present day deformation and its relationships with the recent magmatism and seismicity less well understood. To unravel some of these aspects, geophysical models of the earth structure, compatible with independent gravity, heat-flow, petrological and geochemical data, that provide enough resolving power to the investigated deformation are required.

We study the contemporary continental tectonic stress along a west-east transect crossing the whole Peninsula from the Tyrrhenian coast, via the Umbria-Marche geological domain, to the Adriatic coast. We make use of a recently published crust/lithosphere-asthenosphere structural earth model [*Chimera et al., 2003*]. Although external forces must have been important in the building up of the North-Central Apennines, we investigate the contribution of internal buoyancy forces with respect to the ongoing slow and complex lithospheric deformations, as revealed by very recent GPS solutions and by the unusual intermediate depth seismicity distribution [*Selvaggi and Amato, 1992*] that does not define a classical Benioff zone. Our study brings additional constraints to the recent magmatism [*Peccerillo, 2002*] observed in Tuscany and highlights the importance of gravitational body forces in the geodynamics of the Central Mediterranean.

Set up of the numerical models

The earth model we use is the S-wave velocity model by Chimera et al. [*2003*] retrieved by using deep seismic sounding profiles, crossing the whole Peninsula [*Pialli et al., 1998*] from the Tyrrhenian via the Tuscan Metamorphic Complex (TMC) and the Umbria-Marche geological domain (UMD) [*Bally et al., 1986*] to the Adriatic, as a priori constraints of new shallow and deep tomographic inversions of surface waves. The retrieved crust and lithospheric mantle (lid) exhibit lateral variation in thickness. Lithospheric roots, more than 120 km wide, between the TMC and UMD, reach a depth of at least 130 km. A sharp and well-developed low-velocity zone in the uppermost mantle (mantle wedge), from the Tyrrhenian dying out beneath the Apennines, separates crust and lid. The lateral variation in the Moho geometry by Chimera et al. [*2003*] is in agreement with the one computed by Agostinetti et al. [*2002*] using receiver functions from broad-band seismic stations beneath the same study transect.

In the uppermost 50 km of the model given in Fig. 1, we use density values estimated from a high-resolution gravimetry survey [*Marson et al., 1998*] made along the study profile. For the deeper structures we convert the S-wave velocity model [*Chimera et al., 2003*] into density [*Ludwig et al., 1970*] considering temperature effects. The concordance between the gravity anomaly directly computed from our density model (no data fitting) and the observed Bouguer anomaly (Fig. 1) is a measure of the reliability of our assumptions linked to the density estimates. Doing so, we fix the density and geometry of the crust-mantle structure, and the viscosity is the only variable parameter in our models.

Viscosity is an important physical parameter in stress modeling, because it influences the stress state and results in strengthening or weakening of Earth's material. The viscosity model of the UMD crust is consistent with the findings of Aoudia et al. [*2003*] computed from the viscoelastic relaxation of the 1997 Umbria-Marche normal faulting earthquake sequence. Being the least-known physical parameter of the model, the effective viscosity of the lithospheric mantle beneath the UMD can be constrained considering the observed regional strain rates. Sub-crustal earthquakes in the region provide an indirect measure of the rate of strain release within the seismogenic body. To compute the observed seismic moment released beneath the UMD in the depth range 30 - 80 km, we used the Harvard Centroid-Moment Tensor Catalog (1977-2002) which contains events with M≥5. Two large shocks occurred in the region: in 19.09.1979 (M_W=5.8) and in 26.03.1998

(M_W=5.4). The remaining UMD sub-crustal earthquakes have lower magnitudes, and their contribution to the cumulative seismic moment release (CSMR) is very low. The CSMR is estimated to be about 8.5×10^{17} N m for the region. Using Kostrov's formula the strain rate, within a volume V (50 km × 50 km × 50 km) over a time interval t (20 years), is 8.5×10^{-17} s^{-1}. This strain rate is used as a constraint on the viscosity of the lid in our test computations vs. the modeled strain rate for various viscosity ratios between lid and asthenosphere. Based on these tests we adopted the effective viscosity of the lid beneath the UMD to be 5×10^{22} Pa s.

To constrain the lateral variation in the viscosity of the lithosphere (Fig. 2), we converted the S-wave velocity model of Chimera et al. [*2003*] to temperature using an approach similar to Goes et al. [*2000*] with a variable compositional rock structure as given in Peccerillo [*2002*].

Slow viscous flow and tectonic (deviatoric) stress are found from the momentum conservation and continuity equations. By defining the stream function ψ as a velocity potential $\mathbf{v} = (\partial\psi/\partial x_2, -\partial\psi/\partial x_1)^{\mathrm{T}}$ the governing equations can be combined to form:

$$\left(\frac{\partial^2}{\partial x_2^2} - \frac{\partial^2}{\partial x_1^2}\right)\eta\left(\frac{\partial^2\psi}{\partial x_2^2} - \frac{\partial^2\psi}{\partial x_1^2}\right) + 4\frac{\partial^2}{\partial x_1 \partial x_2}\eta\frac{\partial^2\psi}{\partial x_1 \partial x_2} = -g\frac{\partial\rho}{\partial x_1} \quad (1)$$

Here (x_1, x_2), ρ, η, and g are the Cartesian co-ordinates, density, viscosity, and acceleration due to gravity, respectively. The equations are solved together with the appropriate boundary and initial conditions. A two-dimensional Eulerian finite element approach [*Naimark et al., 1998*] is used to solve the corresponding discrete problem derived from Eq. (1). This is based on the Galerkin method and bi-cubic spline interpolations of unknown variables. The method has been successfully applied to model stress field in a descending slab [*e.g. Ismail-Zadeh et al., 2000*].

The maximum shear stress is determined from the computed components of the tectonic stress tensor τ_{ij} $(i, j = x_1, x_2)$:

$$\tau_{\max} = \left[\frac{1}{2}\left(\tau_{11}^2 + \tau_{22}^2 + 2\tau_{12}^2\right)\right]^{1/2} = \eta\left[4\left(\frac{\partial^2\psi}{\partial x_1 \partial x_2}\right)^2 + \left(\frac{\partial^2\psi}{\partial x_2^2} - \frac{\partial^2\psi}{\partial x_1^2}\right)^2\right]^{1/2} \quad (2)$$

To minimize boundary effects, the studied cross-section has been extended along the horizontal (100 km leftward and 100 km rightward) and vertical (10 km upward and 190 km downward) directions. We prescribe free slip conditions at the boundary of this extended model domain. We use zero-density and 10^{15} Pa s viscosity for the layer above the seismic section as an approximation to the physical parameters of air. Horizontally and downward, the density and viscosity of the extended regions are kept constant and equal to that at the relevant portion of the boundary of the cross-section. The model domain is divided into 98x94 elements in the horizontal and vertical directions, with a spatial resolution of 4.46 km $\times$ 4.89 km.

Model results

The modeled flow field responds directly to the density and viscosity distributions (Fig. 2). The motion of the crust and mantle is caused by the negative buoyancy of the lid and the positive buoyancy of the mantle wedge. The downward motion due to the denser lid sinking in the mantle can be responsible for the subsidence of the Adriatic realm, and the up-welling predicted at the western part of the profile contributes to the tectonic uplift in Tuscany, where the horst-graben structure is observed. Therefore the predicted flow field is in agreement with the regional geological observations [*Pialli et al, 1998*].

The velocities predicted by the numerical model in the upper crust of the region (about 3 mm yr^{-1} as a maximum horizontal velocity at the surface) correlate in magnitude with the preliminary results from the two continuous GPS stations CAME and ELBA (Fig. 1) we deliberately installed, in late 2000, along the transect to monitor the ongoing continental deformation [Gardi et al., 2003]. CAME (Camerino) and ELBA (Elba Island) stations are located at both edges of the continental extension. CAME is right in-between the juxtaposed extension and compression. The CAME-ELBA baseline computed from the ASImed (geodaf.mt.asi.it) GPS-VLBI-SLR combined solution is extending at a rate of 2.6 ± 2.3 mm yr^{-1} [*Devoti, personal communication*].

The computed upward and downward flow field, visible in the western and the eastern parts of the transect, respectively, is well in agreement with the sharp decrease of the heat flow values from west to east (Fig. 2). The horizontal eastward flow field observed within the low velocity mantle wedge (between 0 and 150 km distance, Fig. 2) that decouples the crust from the lid (between 30 and 50 km depth, Fig. 2) is compatible with a delamination process and it may explain the mantle wedge emplacement. The magmatic rocks, at the surface, rich in incompatible elements and their crustal-like isotopic signatures consistent with a genesis in a sub-crustal anomalous mantle [*Peccerillo, 2002*], and the high heat flow values (in agreement with the computed upward flow field) suggest that this mantle wedge is a partially molten mantle that feeds the TMC. The clear decrease in the ages of the TMC rocks ranging from 8-7 to 0.2 Ma from west to east along the transect [*Peccerillo, 2002*], is compatible with the predicted eastward flow in the mantle wedge.

As shown in Fig. 2, the lateral variation in the viscosity of the lithosphere corresponds to the rather sharp heat flow difference (> 100 mW/m^2) observed in the area. To test the stability of our results (Fig. 3) we consider three models of viscosity profiles: (i) model *a* viscosity distribution is shown in Fig. 2; (ii) in model *b* the effective viscosity of the TMC upper crust is less than that in model *a* by a factor of 5; and (iii) in model *c*, the effective viscosity of the UMD upper crust is higher than that in model *a* by a factor of 5. Figure 3 shows the state of tectonic stress in the study transect. A decrease in the effective viscosity of the upper crust beneath TMC does not affect strongly the stress field (compare *a* and *b*). The higher effective viscosity of the upper crust beneath the UMD, the larger shear stress (*c*). The maximum horizontal compressional stress is associated with the lid below the UMD, in the depth range from 50 to 80 km. This finding is in good agreement with the compressional mechanisms of well-constrained fault-plane solutions [*Selvaggi and Amato, 1992*]. The region of high shear stress in the models correlates well with the distribution of the sub-crustal seismicity reported in the literature [*e.g. Chimera et al., 2003*]. The puzzling hypocenter location of the sub-crustal seismicity, which does not define a Wadati-Benioff seismic zone, can now be explained by the particular geometry and buoyancy of the delaminating lithosphere. In the crust the models predict compressional regime at the eastern part of the profile, as already reported in the literature, and tension just below the Umbria-Marche Apennines, where the 1997 normal faulting earthquake sequence took place. Our stress models predict tension below the Quaternary extensional sedimentary basins (Fig. 3) as well. The crust exhibits tension where the TMC outcrops and where the underlying mantle wedge and the asthenospheric low velocity layer are uprisen. This localized uplift-subsidence type of motion is in agreement with a radial extension in proximity of Quaternary vertical intrusions [*Patacca and Scandone, 1989*]. The geoid, with a centimeter precision [*Barzaghi et al., 2002*], that is a proxy for the amount of gravitational potential energy (GPE) available to drive deformation in the lithosphere, exhibits its steepest gradient (Fig. 3) where the lithosphere is highly deformed (km 150-200 distance, Fig 3). The deformation patterns, either observed or modeled, are spatially correlated with GPE patterns.

Conclusions and discussion

We have shown here that the buoyancy forces that result from the density distribution in the lithosphere govern the present day deformation within North-Central Italy and can explain regional coexisting contraction and extension and the shallow depth and unusual distribution of intermediate depth earthquakes. The modeled uppermost mantle flow supports the lithospheric delamination beneath the peninsula and provides a unifying background for petrological and geochemical studies of recent magmatism and volcanism in Tuscany.

The reported unchanged time-space stress field, inferred from the magnetic anisotropy of Plio-Pleistocene sediments [*Sagnotti et al., 1999*] in the compressional part, and the distribution of the thick extensional Quaternary sedimentary basins, in places where our model predicts high magnitude tension, makes us think that buoyancy is the prevailing mechanism in this slow-rate deforming area since, at least, Pleistocene times. This is further supported by the compatibility between the eastward flow within the mantle wedge delaminating the lid from the crust and the clear eastward decrease in the ages of the Plio-Quaternary magmatism (8-7Ma – 0.2Ma).

Acknowledgments. The work benefited from discussions with R. Barzaghi, R. Devoti and A. Peccerillo. Constructive criticism by G. Houseman substantially improved an initial version of the manuscript. We thank two anonymous reviewers for their helpful comments. This research was funded by Italian MIUR Cofin-2002. A.T.I-Z was supported by the Alexander von Humboldt-Stiftung.

References

Agostinetti, N. P., F. P. Lucente, G. Selvaggi, and M. Di Bona, Crustal structure and Moho geometry beneath the Northern Apennines (Italy), *Geophys. Res. Lett., 29 (20)*, 60-1/4, 2002.

Aoudia, A., et al., Postseismic deformation following the 1997 Umbria-Marche (Italy) moderate normal faulting earthquakes, *Geophys. Res. Lett., 70*, 1390-1393, 2003.

Barzaghi, R., B. Betti, A. Borghi, G. Sona, and V. Tornatore. The Italian quasi-geoid ITALGEO99. *Bollettino di Geodesia e Scienze Affini, 1*, 33-51, 2002.

Bally, A.W., L. Burbi, C. Cooper, and R. Ghelardoni, Balanced sections and seismic reflection profiles across the Central Apennines, *Mem. Soc. Geol. It., 35*, 257-310, 1986..

Chimera, G., A. Aoudia, A. Sarao', and G.F. Panza, Active Tectonics in Central Italy: constraints from surface wave tomography and source moment tensor inversion, *Phys. Earth Planet. Inter., 138*, 241-262, 2003.

Gardi, A., R. Sabadini, C. Ferraro, and A. Aoudia, The interplay between global tectonic processes and the seismic cycle in the Umbria–Marche seismogenic region, *Geophys. J. Int., 155*, 1093 – 1104, 2003.

Goes, S., R. Govers, and P. Vacher, Shallow mantle temperatures under Europe from *P* and *S* wave tomography. *J. Geophys. Res.* 105, 111, 53-11169, 2000.

Della Vedova, B., S. Bellani, G. Pellis, and P. Squarci, In: Vai, G.B., and Martini, I.P., (Editors). *Anatomy of an Orogen*: the Apennines and Adjacent Mediterranean Basins. Kluwer Academic Publisher, 65-76, 2001.

Doglioni, C., P. Harabaglia, S. Merlini, F. Mongelli, A. Peccerillo, and C. Piromallo, Orogens and slabs vs. their direction of subduction. *Earth-Science Reviews, 45*, 167-208, 1999.

Frepoli, A., and A. Amato, Contemporaneous extension and compression in the Northern Apennines from earthquake fault-plane solutions, *Geophys. J. Int., 129*, 368-388, 1997.

Ismail-Zadeh, A.T., G.F. Panza, and B. N. Naimark, Stress in the descending relic slab beneath the Vrancea region, Romania, *Pure Appl. Geophys. 157*, 111-130, 2000.

Ludwig, W.J., J.E. Nafe, and C.L. Drake, In: Maxwell, A.E., (Editor). *New concepts of sea floor evolution*. Wiley-Interscience, New York: 53-84, 1970.

Marson, I., L. Cernobori, R. Nicolich, M. Stoka, D. Liotta, F. Palmieri, and I. Velicogna, CROP-03 profile: a geophysical analysis of data and results, *Mem. Soc. Geol. It., 52*, 123-137, 1998.

Montone, P., A. Amato, and S. Pondrelli, Active stress map of Italy, *J. Geophys. Res. 104*, 25595-25610, 1999.

Naimark, B.N., A.T. Ismail-Zadeh, and W.R. Jacoby, Numerical approach to problems of gravitational instability of geostructures with advected material boundaries, *Geophys. J. Int.* 134, 473-483, 1998.

Negredo, A.M., S. Barba, E. Carminati, R. Sabadini, and C. Giunchi, Contribution of numeric dynamic modelling to the

understanding of the seismotectonic regime of the Northern Apennines, *Tectonophysics, 315*, 15-30, 1999.
Patacca, E. and P. Scandone, In: The lithosphere in Italy. (eds Boriani et al.) 157-176 (Acc. Naz. Lincei., 80), 1989.
Peccerillo, A., Quaternary magmatism in central-southern Italy: a new classification scheme for volcanic provinces and its geodynamic implications, *Boll. Soc. Geol. It.*, 1, 113-127, 2002.
Pialli, G., M. Barchi, and G. Minelli (eds), Results of the CROP03 Deep Seismic Reflection Profile, *Mem. Soc. Geol. It.*, *LII*, 657 pp., 1998.
Sagnotti *et al*. Magnetic anisotropy of Plio-Pleistocene sediments from the Adriatic margin of the northern Apennines (Italy): implications for the time-space evolution of the stress field. *Tectonophysics*, 311, 139-153, 1999.
Selvaggi, G., and A. Amato, Subcrustal earthquakes in the Northern Apennines (Italy): evidence for a still active subduction? *Geophys. Res. Lett.*, 19, 2127-2130, 1992.
Wortel, M.J.R., and W. Spakman, Subduction and slab detachment in the Mediterranean-Carpathian region. *Science, 290*, 1910-1917, 2000.

A. Aoudia, G.F. Panza, Abdus Salam International Centre for Theoretical Physics, SAND Group, Trieste, Italy & Dept. of Earth Sciences, University of Trieste, Italy. (e-mail: aoudia@dst.units.it, panza@dst.units.it)
A. T. Ismail-Zadeh, International Institute of Earthquake Prediction Theory and Mathematical Geophysics, Russian Academy of Sciences, Moscow, Russia & Geophysikalisches Institut, Universität Karlsruhe, Germany (e-mail:. Alik.Ismail-Zadeh@gpi.uni-karlsruhe.de).

(Received ?, 2004; revised ?,?; accepted ?, ?)

AOUDIA ET AL.: BUOYANCY-DRIVEN DEFORMATIONS

AOUDIA ET AL.: BUOYANCY-DRIVEN DEFORMATIONS

Figure 1.
(a) Density model of the crust and uppermost mantle beneath North-Central Italy and the hypocentres of the sub-crustal earthquakes (vertical bars indicate the depth error) recorded in the period 1965-1998 (Selvaggi and Amato, 1992; ISC) within a stripe 150 km wide along the study profile (red line in the inset). The study profile, from the Tyrrhenian to the Adriatic coastlines, crosses the Tuscan Metamorphic Complex (TMC) and the Umbria-Marche geological Domain (UMD). The bold black segment indicates the Moho depth (Chimera et al. 2003). The topmost line presents the surface topography.
(b) Observed (Marson et al., 1998) Bouguer gravity anomaly (blue) vs. gravity (red) predicted from our density model.
(**c, d**) study profile and schematic geological model after Patacca and Scandone (1989) and locations of continuous GPS stations.

Figure 2.
Effective viscosity used and predicted flow field (bottom panel). A reduction of the effective viscosity of the crust and mantle lithosphere at the left of the model correlates with a high heat flow observed in the region (Della

Vedova et al., 2001 - upper panel) and with the recent magmatism (Peccerillo, 2002).

Figure 3.
Tectonic shear stress and compressional axes (ticks) predicted by models (a), (b) and (c) along the studied profile (tensional axes are perpendicular to the compressional ones). The horizontal ticks indicate thrusting and vertical ticks indicate normal faulting. The viscosity profile for model (a) is shown in Fig. 2. See text for models (b) & (c). The geoid height computed from Barzaghi et al. (2002) exhibits its steepest gradient along the study profile and above the area of maximum deformation predicted in model (a).

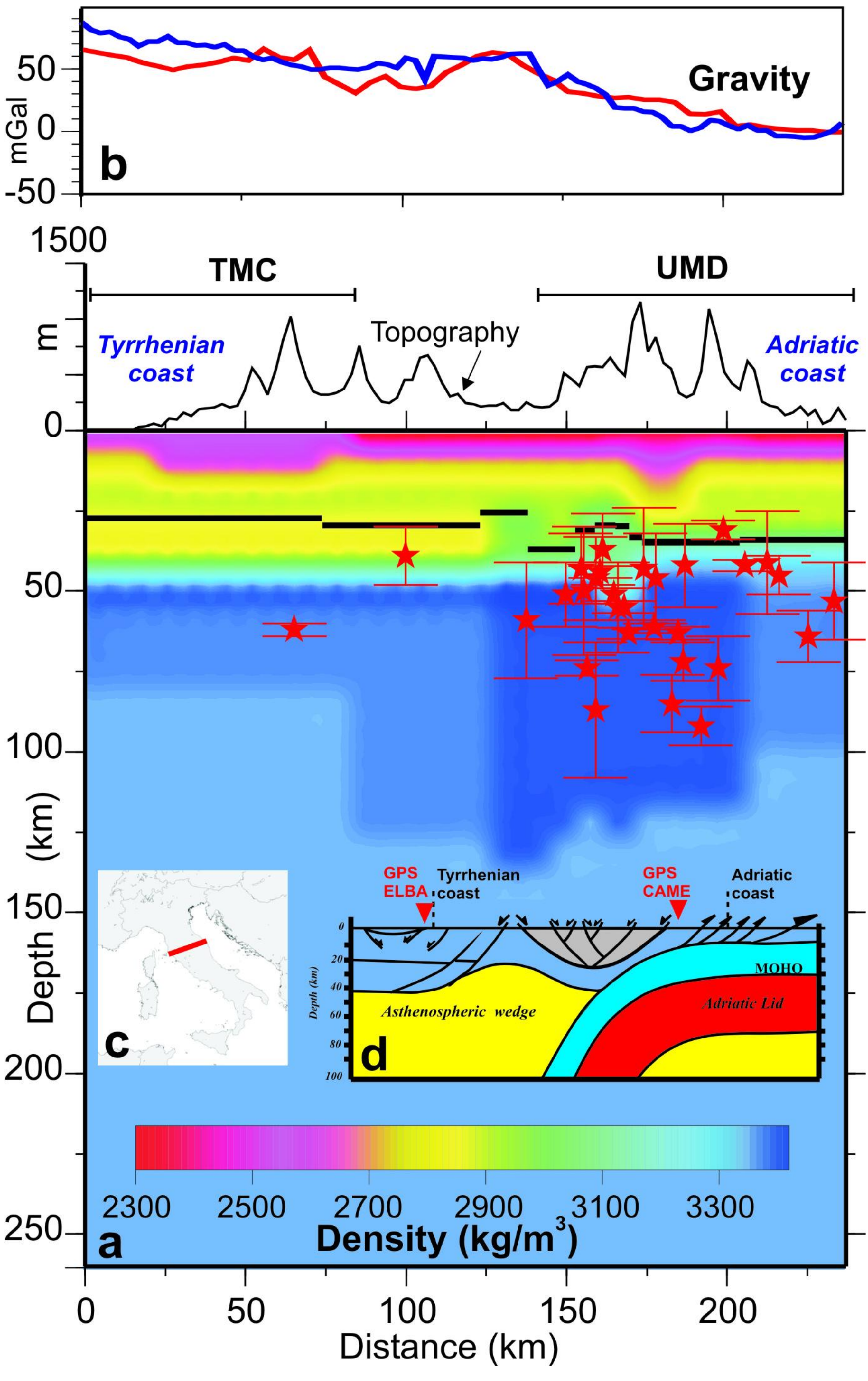

Gravity
mGal
b
TMC
UMD
m
Topography
Tyrrhenian coast
Adriatic coast
Depth (km)
GPS ELBA
Tyrrhenian coast
GPS CAME
Adriatic coast
Depth (km)
MOHO
Asthenospheric wedge
Adriatic Lid
c
d
Density (kg/m^3)
a
Distance (km)

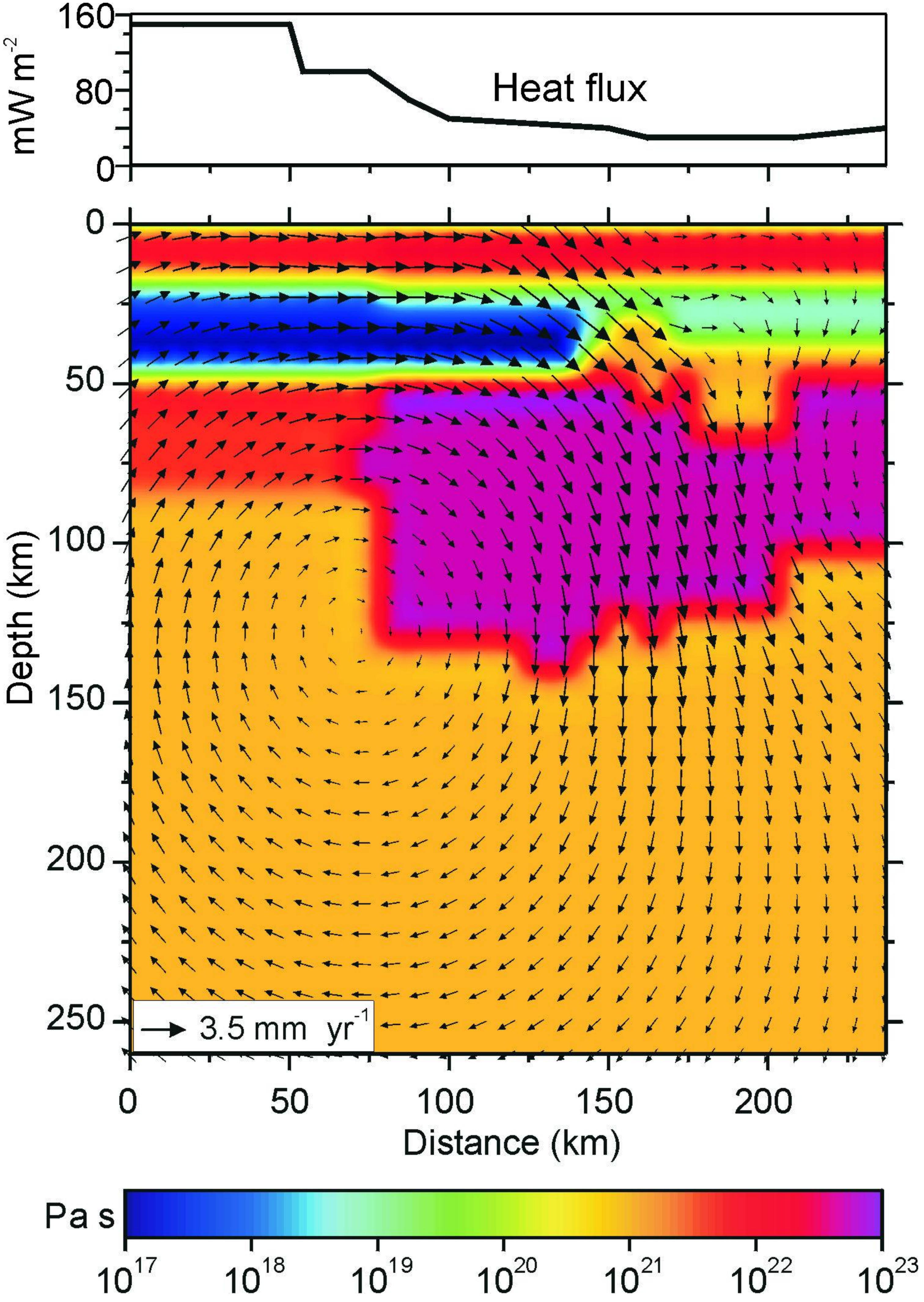

Heat flux
$mW\,m^{-2}$
160
80
0
Depth (km)
0
50
100
150
200
250
3.5 mm yr^{-1}
0
50
100
150
200
Distance (km)
Pa s
10^{17}
10^{18}
10^{19}
10^{20}
10^{21}
10^{22}
10^{23}

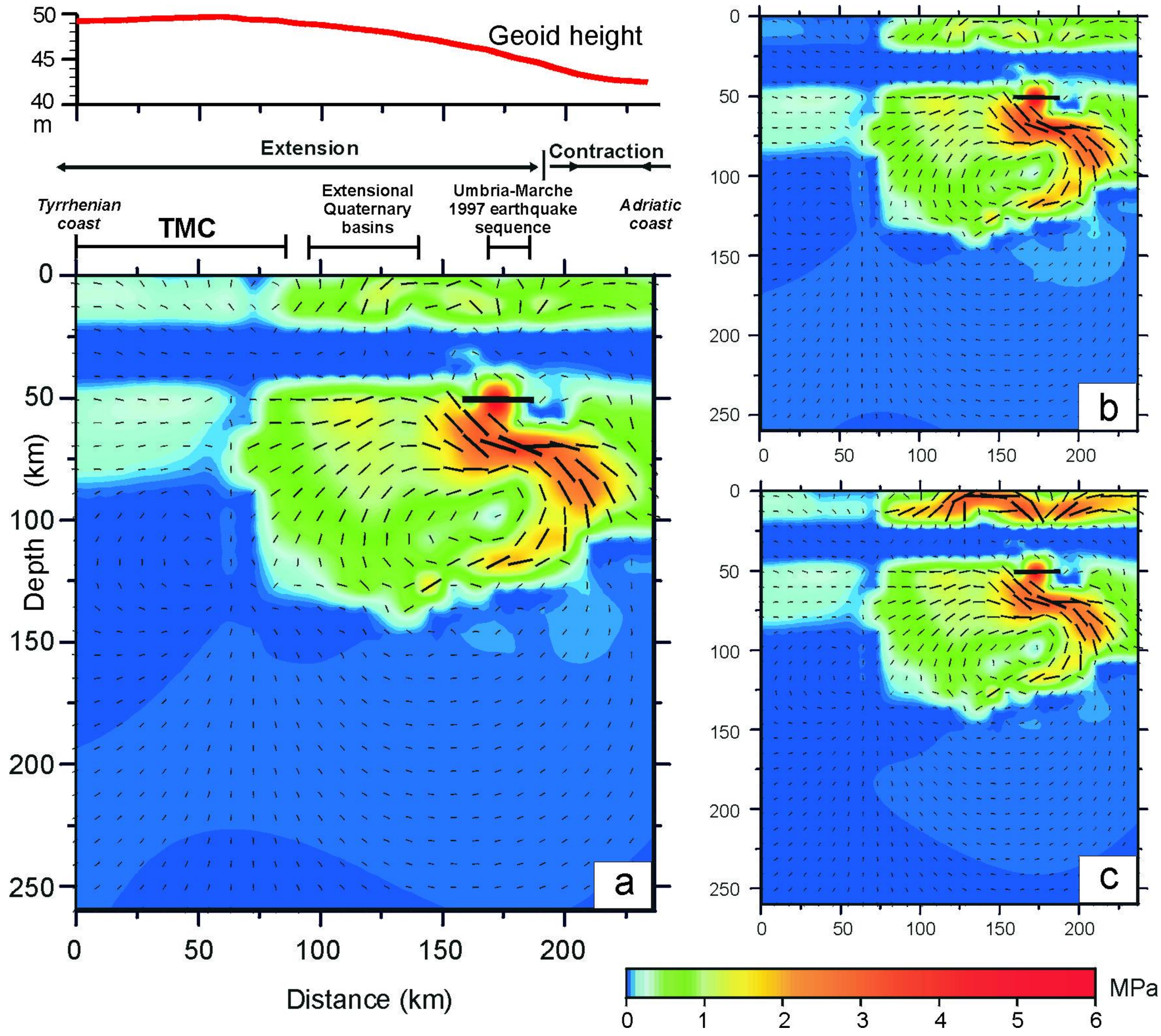

Geoid height
m
Extension
Contraction
Tyrrhenian coast
TMC
Extensional Quaternary basins
Umbria-Marche 1997 earthquake sequence
Adriatic coast
Depth (km)
Distance (km)
a
b
c
MPa